Title: Studies on structurally different benzoxazines based on diphenols and diamines: kinetics of thermal degradation and TG-FTIR studies

Author: S. Shamim Rishwana A. Mahendran C.T. Vijayakumar

PII: S0040-6031(15)00362-7
DOI: http://dx.doi.org/doi:10.1016/j.tca.2015.09.006
Reference: TCA 77341

To appear in: *Thermochimica Acta*

Received date: 2-6-2015
Revised date: 4-8-2015
Accepted date: 5-9-2015

Please cite this article as: S.S. Rishwana, C.T. Vijayakumar, Studies on structurally different benzoxazines based on diphenols and diamines: kinetics of thermal degradation and TG-FTIR studies, *Thermochimica Acta* (2015), http://dx.doi.org/10.1016/j.tca.2015.09.006

Highlights

1. Aromatic diphenol and diamine based bisbenzoxazines were prepared and polymerized

2. Polybisbenzoxazines from Quinol and p-phenylenediamine results in ladder structures

3. Meta diphenol and diamine based materials show intramolecular hydrogen bonding

4. Para oriented materials show higher thermal stability than meta oriented materials

5. Phenols are the major degradation products from diphenol based polybisbenzoxazines

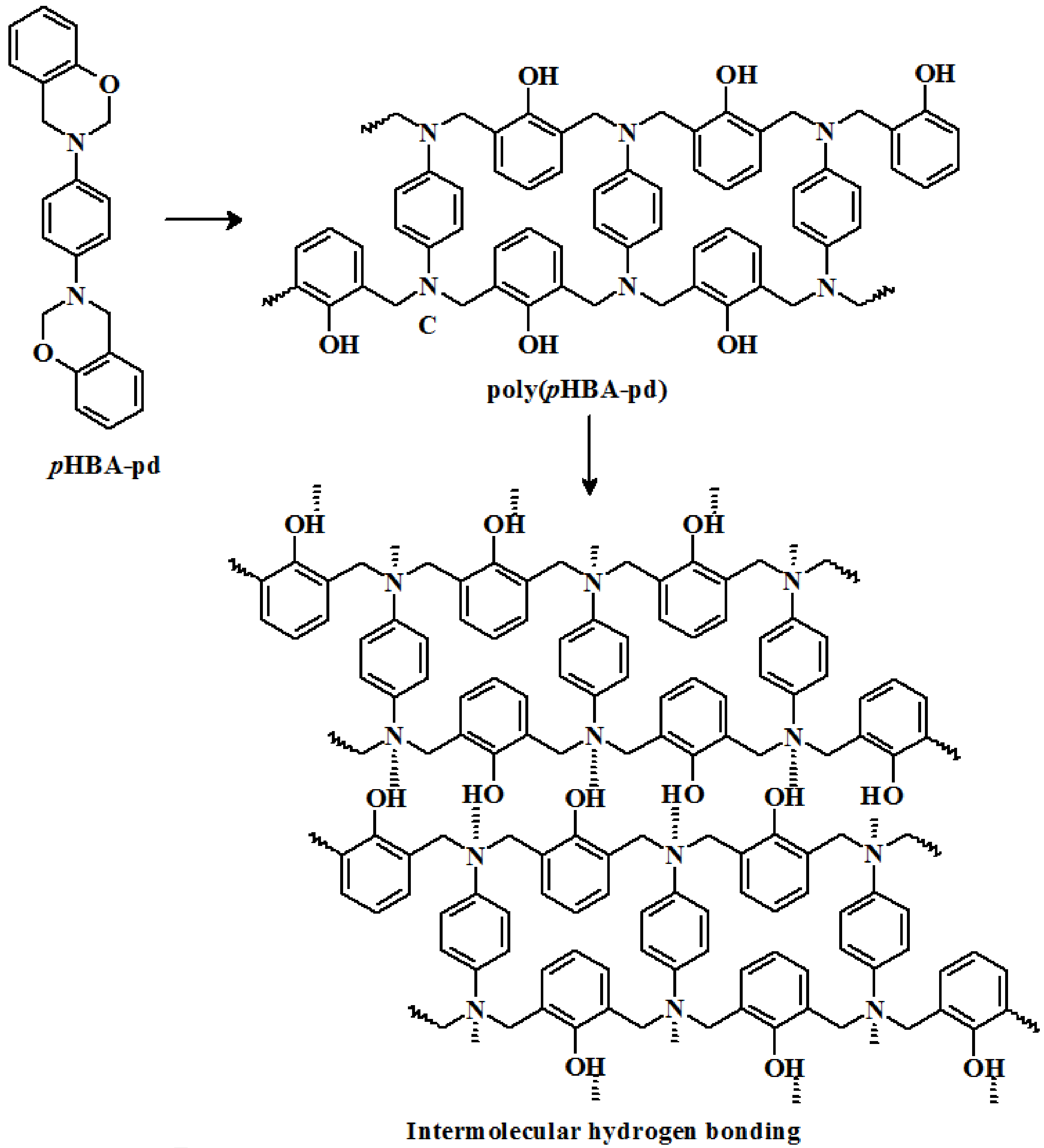
O
N
N
O
*p*HBA-pd
OH
OH
OH
N
N
N
N
N
N
C
OH
OH
OH
poly(*p*HBA-pd)
Intermolecular hydrogen bonding

Studies on structurally different benzoxazines based on diphenols and diamines: kinetics of thermal degradation and TG-FTIR studies.

S. Shamim Rishwana[1], A.Mahendran[2], C. T. Vijayakumar[3]*

[1]Department of Chemistry, Kamaraj College of Engineering and Technology,
K. Vellakulam Post 625 701, India

[2]Competence Center for Wood Composites and Wood Chemistry Ltd, Area Wood Carinthian Competence Center (W3C), Klagenfurterstrasse 87-89, St. Veitan der Glan, Austria.

[3]Department of Polymer Technology, Kamaraj College of Engineering and Technology,
K. Vellakulam Post 625 701, India

Paper submitted for publication in
Thermochimica Acta

*Author to whom correspondence should be addressed.
Tel.: +91 94420 57674
E-mail: ctvijay22@yahoo.com

Abstract

Structurally different bisbenzoxazines(QB, RB, *p*HBA-pd and *m*HBA-pd) are synthesized using quinol, resorcinol, *p*-phenylenediamine and *m*-phenylenediamine and are thermally cured. The thermal stability of the materials was studied using TGA. The plate like structure resulting from the interlinking of the ladders by intermolecular hydrogen bonding provides thermal stability to poly(*p*HBA-pd). The kinetics of thermal degradation is followed using Vyazovkin and Friedman methods. The diphenol based polybisbenzoxazines show higher apparent activation energy for thermal degradation (Ea-D) (PQB =252 to 330 kJ/mol) than the diamine based polybisbenzoxazines (poly(*p*HBA-pd) = 98 to188 kJ/mol). Aromatic amines are found to be released in considerable quantities from the diamine based polybisbenzoxazines whereas phenolics are released from diphenol based polybisbenzoxazines.

Keywords

Bisphenols, aromatic diamines, bisbenzoxazines, FTIR, TGA, Model free kinetics, TG-FTIR.

1. Introduction

Phenolic resins [1] are playing a key role on the thermosetting resin market since they appeared in the early twentieth century. They are widely used for a variety of applications including high performance materials for aerospace industry. Phenolic resins possess such important advantages as good mechanical strength, dimensional stability, chemical resistance and flame retardance. However, they are associated with the drawbacks of traditional phenolic resins such as release of volatiles upon curing which results in micro voids in composite matrix and need for strong acid as a crosslinking catalyst. Thus, phenolic resins provide some challenges for the development of the products with desirable properties and industrial production.

Due to the reasons described above, polybisbenzoxazines, a newly developed class of thermosetting resins, recently are getting strong attention since they combine the advantages of phenolic resins and it is one of the very few new classes of polymers which were successfully commercialized in the last three decades.

Benzoxazine monomers are heterocyclic compounds obtained *via* condensation of an amine, formaldehyde and a phenol and were first synthesized by Holly and Cope [2]. Benzoxazine resins [3-5]have a wide range of mechanical and physical properties that can be tailored to various needs, reflecting the extremely rich molecular design flexibility. The material property balance of polybenzoxazines is excellent. Good thermal, chemical, electrical, mechanical and physical properties make them attractive alternatives to existing applications. Additional new applications can be developed by utilizing unique properties of polybenzoxazines that have not been often observed by other well known polymers. Those properties include near-zero shrinkage, very high char yield, fast development of mechanical properties as a function of conversion, glass transitions, much higher than curing temperatures, excellent electrical properties and low water uptake despite having many hydrophilic groups.

Bisbenzoxazines can be synthesized from inexpensive raw materials and polymerized by a ring-opening addition reaction, yielding no reaction by-product. The superb molecular design flexibility of the polybenzoxazines allows the properties of the polymerized materials to be tailored in a wide range of properties for the specific requirements of individual applications. Reiss et al.[6]studied the reaction kinetics of benzoxazine oligomer formation using, mostly the mono functional benzoxazines, showing that large molecular weight linear polybenzoxazines cannot be obtained from mono functional benzoxazines. Several monomers studied showed the molecular weights roughly between a few hundreds to a few thousands upon polymerization.

In the present investigation the authors studied the properties of different bisbenzoxazines having similar molecular formula by choosing hydroquinone (Q), resorcinol (R), *p*-phenylenediamine (PPDA) and *m*-phenylenediamine (MPDA) as the reactants. The hydroquinone and resorcinol based bisbenzoxazines have been prepared by solvent method whereas *p*-phenylenediamine and *m*-phenylenediamine based bisbenzoxazines are prepared by three step process [7]. The full names and abbreviated names of the materials used are given in Table 1

Table 1

Thermogravimetric studies (TG) provide information regarding composition of multi-component materials or blends, thermal stability, oxidative stability, estimation of product life time, effect of reactive atmosphere on material, filler content in materials, moisture and volatiles content and decomposition kinetics of the polymeric materials [3]. Non-isothermal method is an easy method to derive the degradation kinetic parameters [4] provided the TG curves recorded at different heating rates are available. In this process, the data necessary for the kinetic analysis can be obtained in a relatively short period of time, although getting the kinetic parameters from these data need complicated mathematical analysis[5]. Generally different mathematical approximations developed Vyazovkin (VYZ) [8-13] and Friedman (FRD) [14] is employed by various authors to derive kinetic parameters from TG data. The use of the expressions developed by Kissinger [15] and Coats-Redfern [16] are also found in the literature.

Thermogravimetric analyzer (TGA) interfaced with Fourier transform infrared spectrophotometer (FTIR) provide information on thermal degradation products [17–20]. Further details about the type and functionality of the degradation products as a function of time and/or temperature [17, 18] can be obtained from TG-FTIR studies. The thermal degradation processes of various polybenzoxazines were studied and the degradation mechanisms were proposed in the literature [21-25]. In the previous investigation [26, 27], bisphenol-A bisbenzoxazine (BAB), indane bisphenol bisbenzoxazine (IBPB) and spirobiindane bisphenol bisbenzoxazine (SBIB) were prepared. The curing of the monomers and thermal stabilities of the cured compounds has been studied. The presence of different structural entities in between the benzoxazine units and the choice of the temperature for the thermal curing have significant effects on the thermal stability of the cross linked polymer.

The structural effects of diphenol and diamine based polybisbenzoxazine on the thermal degradation of polybisbenzoxazines were not investigated systematically and discussed. Hence the authors studied the thermal curing kinetics of these compounds and reported in the previous paper [7]. The results showed that the para substituted aromatic compounds based bisbenzoxazines show higher apparent activation energy for curing (Ea-C) in the initial curing stage. This reveals that, not only the structure and molecular formula of the compound determines the characteristics of the polymers, the nature of the oxazine ring formed will also play a vital role in the curing of the monomers. Here in the present investigation, the authors intended to investigate in detail the apparent activation energies for the degradation (Ea-D) of the different polybisbenzoxazine thermosets and the results will be discussed in light of the structure of the materials. The volatile products formed during the thermal degradation of these compounds have also been studied using TG-FTIR and the results are presented and discussed.

2. Experimental

2.1 Materials

Bisphenol-A and paraformaldehyde were purchased from SISCO Research Laboratory Pvt. Ltd., Mumbai-400099. Sodium hydroxide, resorcinol, quinol, ethanol and 1,4-dioxane were purchased from Lobachemie Pvt. Ltd, Mumbai-400002. Sodium borohydride was purchased from S.D. fine chem Ltd., Mumbai-400025. Aniline, *m*-phenylenediamine, *p*-phenylenediamine, 2-hydroxybenz-aldehyde (HB), N,N'-dimethylformaldehyde (DMF), chloroform and diethylether were purchased from MERCK Specialist Pvt. Ltd, Mumbai-400018. Aniline and 1,4-dioxane were distilled and used.

2.2 Preparation of 3,3′-(*p*-Phenylene)bis(3,4-dihydro-2*H*-1,3-benzoxazine)(*p*HBA-pd) and 3,3′-(*m*-Phenylene)bis(3,4-dihydro-2*H*-1,3-benzoxazine) (*m*HBA-pd)

An aromatic diamine PPDA was employed as a material to form *p*HBA-pd by using the 3-step process [28].

Step (I): 2-Hydroxybenzaldehyde (0.12 mol = 14.6 g) and 0.06 mol (6.5 g) of PPDA were taken in a 250mL round bottomed flask and dissolved in 100mL of DMF with efficient stirring. The solution was kept at room temperature and stirred for three hours; the formed precipitate was filtered and dried for 24 h in an air oven kept at 80 °C to obtain the first intermediate (PPDA-HB) in powder form.

Step (II): Nitrogen was introduced into a reactor to remove the humidity for 30 minutes and a balloon with hydrogen was assembled on the reactor. The first intermediate (PPDA-HB, 0.03 mol = 9.5 g) was dissolved in 30mL of ethanol and added to the reactor. Sodium borohydride (0.075 mol = 2.5 g) was divided into 3 batches and added into the reactant and the contents were kept at room temperature and stirred for 10 hours. The mixture was added into water to precipitate. The precipitate is filtered and dried for 24 h in an air oven kept at 80 °C to obtain the second intermediate (PPDA-HB-r).

Step (III): In a 250 mL round flask the second intermediate (PPDA-HB-r, 0.03 mol = 9.6 g) was dissolved in 85mL of chloroform. Formaldehyde solution (0.06 mol = 4.6 mL) was added to the above solution in drop wise and the mixture was stirred for 4 hours at room temperature. The temperature was increased and the solution was refluxed for 5 hours. The solution was added into the ethanol solution (ethanol:water = 1:1) to precipitate the bisbenzoxazine (*p*HBA-pd) Scheme 1. The *m*-phenylenediamine bisbenzoxazine (*m*HBA-pd) was also prepared by employing the same procedure. The materials were dried for 24 h in an air oven kept at 80 °C.

Scheme 1

2.3 Preparation of 3,7-Diphenyl-3,4,7,8-tetrahydro-2H,6H-1,5-dioxa-3,7-diaza-phenanthrene (RB) and 3,6-Diphenyl-2,3,4,5,6,7-hexahydro-1,8-dioxa-3,6-diaza-phenanthrene (QB).

In a 100 mL flask, aniline (0.06 mol, 5.9 g) was dissolved in 25 mL of 1,4-dioxane at room temperature. The solution was cooled in an ice bath, followed by the portion wise addition of paraformaldehyde (0.12 mol, 3.8 g) with stirring for 10 min. Then quinol (0.03 mol, 3.5 g) was added to this cold solution. The temperature was raised and refluxed for 24 h. After removing 1,4-dioxane under vacuum, the resulting crude product was purified by dissolving in 150 mL of diethyl ether and washing several times with 0.1N sodium hydroxide, and finally two times with distilled water. After drying with anhydrous sodium sulfate, the mass was dried under vacuum at 60 °C for 24 h to afford solid [29]. The reaction is presented in Scheme 2

Scheme 2

2.4 Thermal curing

The bisbenzoxazines, QB, RB, *p*HBA-pd and *m*HBA-pd were taken in separate micro test tubes and flushed with dry oxygen-free-nitrogen and thermally polymerized (QB = 210 °C, RB = 225 °C , *p*HBA-pd = 250 °C, and *m*HBA-pd = 140 °C) for 6 hours. After the polymerization, the samples were removed from the micro test tubes, ground to coarse powder, packed and stored for further analysis.

2.5 Methods

Shimadzu (S8400) FTIR spectrophotometer was used for recording the FTIR spectra of bisbenzoxazines and polymerized materials. The KBr disc technique was employed.

2.6 Thermogravimetric analysis (TGA)

The degradation behavior of the polymerized bisbenzoxazines was examined using TGA Model Q50 supplied by TA Instruments. The measurements were carried out using approximately 4-5 mg sample in nitrogen atmosphere and the flow of nitrogen to the balance area was 40 mL/min and sample was swept with a nitrogen flow of 60 mL/min and the materials were heated from 40 to 800°C using different heating rates (5, 10, 20 and 30°C/min).

2.7 TG-FTIR

The TG-FTIR studies were carried out in the instrument TGA Q5000 V3.10 Build 258 purchased from TA Instruments employing a heating rate of 10°C/min from ambient to 900°C under nitrogen atmosphere. The nitrogen flow was 10 mL/min.

2.8 Kinetic studies

The rate of solid-state reactions can be described as

$$\frac{d\alpha}{dt} = k(T)\, f(\alpha) \qquad (1)$$

where dα/dt is the rate of the reaction, k(T) is the rate constant, f(α) is the reaction model[30]. According to Arrhenius's equation, the temperature-dependent rate constant, k(T) is defined as

$$k(T) = A \exp\left(-\frac{Ea}{RT}\right) \qquad (2)$$

where A is the pre-exponential factor, Ea is the apparent activation energy, R is the gas constant and T is the temperature.

The reaction extent (α) for the degradation reaction is shown in the following equation

$$\alpha = \left(\frac{W_o - W_T}{W_o - W_e}\right) \qquad (3)$$

2.8.1 Vyazovkin method (VYZ)

According to Vyazovkin's model free kinetic method, the activation energy can be determined at any particular degree of conversion by finding the value of Ea in Eq. (4) for which the objective function Ω is minimized.

$$\Omega = \sum_{i=1}^{n} \sum_{j=1, j \neq 1}^{n} \frac{I\left(Ea, \ T_{ai}\right)\beta_j}{I\left(Ea, \ T_{aj}\right)\beta_j} \qquad (4)$$

with

$$I\left(Ea, T_{ai}\right)\beta_j = \int_0^{T_a} \exp\left(-\frac{Ea}{RT}\right) dt \qquad (5)$$

Theory and application of model free kinetic approaches, starting from basic rate equations and ending in activation energy prediction is discussed in the literature [31-38]. Since every kinetic method has different error, the use of more than one method can give a range of values for the activation energy at very particular value of the extent of reaction (α).

2.5.3 Friedman method (FRD)

This is one of the differential methods used to calculate Ea and the equation [14] is given below:

$$\ln\left(\frac{d\alpha}{dT}\right) = \ln A + \ln f(\alpha) - \left(\frac{Ea}{RT}\right) \quad (6)$$

$$\ln\left(\frac{d\alpha}{dt}\right) = \ln(z) + n\ln(1-\alpha) - \left(\frac{Ea}{RT}\right) \quad (7)$$

From the slope (-Ea/R) of the linear plot between ln(dα/dt) vs. 1/T, the apparent activation energy (Ea) of the system can be calculated.

3. Results and discussion

3.1 FTIR Studies

The FTIR spectra recorded for the compounds *p*HBA-pd, *m*HBA-pd, QB and RB is presented in Fig 1. The absence of the band at 2908 cm^{-1} in *p*HBA-pd and *m*HBA-pd indicates the $-NH_2$ group present in PPDA and MPDA have been used for the formation of oxazine rings. The condensation reaction of the phenolic (quinol and resorcinol) compounds with aniline and paraformaldehyde resulted in the formation of QB and RB respectively. The absence of the broad absorption peak typical for the –OH group (3500 cm^{-1}) in QB and RB confirms the consumption of the –OH groups and leads to the formation of the monomer. The band noted at 948 cm^{-1} [39-42] is useful to recognize the oxazine ring structure. This band is due to the benzene ring mode of the benzene to which oxazine is attached. Further the presence of the oxazine rings in the prepared compounds was supported by the appearance of new absorption bands for the oxazine asymmetric and symmetric stretching at 1230 and 1500 cm^{-1} respectively. The presence of C_6H_5-N group in QB and RB is confirmed by presence of an absorption band at 2908 cm^{-1}.

Fig 1

The FTIR spectra recorded for the polymers (poly(*p*HBA-pd), poly(*m*HBA-pd), PQB and PRB) are also presented in Fig. 1. The presence of an intense band at 3361 cm^{-1} indicates the formation of phenolic groups during the ring opening polymerization of the benzoxazines. When oxazine ring opens, the band noted at 948 cm^{-1} disappears. It is important to note that disappearance of this mode is not the evidence of oxazine polymerization, but it is a simple indication that the oxazine ring opened [39]. Further, the complete disappearance of the peaks specific for the oxazine group in the FTIR spectrum of the polymers obtained by thermally polymerizing indicates the completion of the thermal polymerization.

Before going into further details, it is necessary to have a look at the different structures resulting from the polymerization of QB, RB, *m*HBA-pd and *p*HBA-pd.

Polymerization of QB results in a ladder like structure (Scheme 3) incorporating the benzene ring in the ladder. The appropriate orientation of the phenyl groups present in the nitrogen atoms is a must to have intermolecular hydrogen bonding (Scheme 3) between the -OH groups present in the periphery of the ladders resulting in a structure that favors much thermal stability.

Polymerization of RB will lead to the formation of the thermoset having the structure shown in Scheme 4. The ring opening followed by polymerization leads to intramolecular hydrogen bonding between the phenolic -OH group and the nitrogen atom of the ortho placed -CH_2-N(-CH_2-)-C_6H_5 unit. Owing to this favorable structure, the polymerization proceeds at the ortho position existing in between the two OH groups. Comparison of the structures of PQB and PRB, one can easily recognize the higher thermal stability of PQB.

Scheme 3

Scheme 4

The ladder structure resulting from the polymerization of *p*HBA-pd is shown in Scheme 5. But the structure is much different from that of the structure noted for PQB. Here the poles of the ladder are joined by phenyl rings and this ladder is much flexible compared to that of the ladder resulting from the polymerization of

QB. As in the case of PQB, the structure resulting from the polymerization of *p*HBA-pd is also amenable for intermolecular hydrogen bonding (Scheme 5) between the ladders through the favorably oriented phenolic -OH groups. Hence poly *p*HBA-pd is comparatively less stable than that of PQB.

Scheme 5

Scheme 6

The structure of the polymer resulting from the polymerization of *m*HBA-pd is presented in Scheme 6. As in the case of PRB, here also the intramolecular hydrogen bonding is present. In this system, the possibilities of the attack at both the ortho and the para positions are shown in Scheme 6. Hence the structures of both *m*HBA-pd and PRB are having considerable amounts of intramolecular hydrogen bonds whereas *p*HBA-pd and PQB are having intermolecular hydrogen bonds.

The materials PQB and poly(*p*HBA-pd) show a band centered at 3418 and 3416 cm^{-1} (Fig 1) respectively and proves the existence of –OH---N intermolecular hydrogen bonding. The polymers PRB and poly(*m*HBA-pd) show significant intramolecular hydrogen bonding as demonstrated by the presence of a strong band at 3400 cm^{-1} (Fig 1). Further the presence of free hydroxyl groups (3615 cm^{-1}) is also noted for these materials.

3.2 TGA and DTG studies:

The TG and DTG traces for poly(*p*HBA-pd), poly(*m*HBA-pd), PQB and PRB recorded at multiple heating rates (10, 20 and 30°C/min) in nitrogen atmosphere are shown in Fig 2. All the thermograms are shifted to higher temperatures with increasing heating rates. The onset, maximum, end set temperatures for the degradation and the char residue obtained at 800 °C for all the samples noted at a heating rate 10 °C/min are tabulated in Table 2.

Fig 2

Table 2

In the previous study [7], the authors reported that the difference in the structure of the bisbenzoxazine influenced the curing behavior of poly(*p*HBA-pd), poly(*m*HBA-pd), PQB and PRB as evidenced by the change noted in the apparent activation energies for the curing of the bisbenzoxazines. Hence, it is reasonable to expect the structural differences must influence the degradation behavior of these materials (poly(*p*HBA-pd), poly(*m*HBA-pd), PQB and PRB).

The detailed observations of the thermogravimetric data for the samples obtained at a heating rate of 10 °C/min are discussed below. The thermally cured pure poly(*p*HBA-pd) shows the onset degradation temperature at 331°C attains maximum at 430°C and ends at 544°C. The DTG curves of thermally cured pure poly(*p*HBA-pd) shows single degradation maximum at 430 °C. The temperature specific for 5% mass loss for poly(*p*HBA-pd) is 369 °C, which is much higher than that of PBAB. According to previous studies, the 5% mass loss temperature of conventional polybenzoxazines rarely exceeds 350 °C and the release of aromatic amines (e.g. aniline) is responsible for the low thermal stability of polybenzoxazines [43-46]. Therefore, the introduction of a cross linkable site in this aromatic amine part, such as ethylnyl [46,47], propargyl ether [48], and nitrile group[49] has been proven to be an effective way to enhance thermal stability of polybenzoxazines. However, an enhanced crosslinking density also indicates a sacrificial toughness .As in Scheme 5, the nitrogen present in poly(*p*HBA-pd) are bonded to the other repeating units and this makes the release of aromatic amines difficult and causing poly(*p*HBA-pd) to be thermally more stable than PBAB.

The poly(*m*HBA-pd) shows three degradation stages and the maxima at 278, 380 and 530 °C. This may be attributed due to the release of different compounds specifically at these stages. This material shows a very low char yield compared to the other materials (poly(*p*HBA-pd), PQB and PRB). The PQB shows a single degradation step. The onset degradation temperature is at 268 °C, attains maximum at 380 °C and ends at 539 °C. The PRB shows three degradation maxima at 310, 330 and 430 °C respectively. Hence the degradation of poly(*m*HBA-pd)and PRB are much complex compared to poly(*p*HBA-pd) and PQB. Further poly(*p*HBA-pd) and PQB are found to be comparatively thermally more stable than poly(*m*HBA-pd)and PRB.

The high initial degradation temperature shown by the material poly(*p*HBA-pd) is mainly due to the structurally favoured intermolecular hydrogen bonding resulting in an interlinking of the ladders leading to a plate like structure. The breaking of the hydrogen bonds followed by further chain scissions leading to the evolution of volatiles is difficult when compared to the intermolecular hydrogen bonding that is present in the case of PQB. Due this fact, the initial degradation temperature of PQB is low. But comparison of the char yield (Table 2) showed that the compound PQB yields slightly higher char than poly(*p*HBA-pd). This may be due to the presence of much flexible ladder structure present in poly(*p*HBA-pd), a situation which favours easy release of volatiles.

3.3 Degradation Kinetic Studies

The apparent activation energy for the thermal degradation of thermally cured materials, poly(*p*HBA-pd), poly(*m*HBA-pd), PQB and PRB, were calculated using three isoconversional model free kinetic methods such as VYZ, and FRD methods. The plots between the apparent activation energy(Ea-D) for thermal degradation and the reaction extent (α) values for all the samples investigated using VYZ, and FRD method are shown in Fig 3.

Fig 3

The trends noted in the variation of apparent activation energy for the degradation of thermally cured samples obtained by the three kinetic methods are same and the values are in good agreement. The slight deviation noted in the apparent activation energy values between these methods is due to the different approximation used in the kinetic methods. The apparent activation energies for thermal degradation obtained using VYZ method for thermally cured poly(*p*HBA-pd), poly(*m*HBA-pd), PQB and PRB is considered for the discussion. The apparent activation energy for the degradation of poly(*p*HBA-pd)increases progressively from 98 to188 kJ/mol. This implies that the degradation of the poly(*p*HBA-pd) follows a similar mechanism throughout the thermal degradation. The apparent activation energy for the degradation of poly(*m*HBA-pd) varies from 92 to 308 kJ/mol. Initially both the compound (poly(*p*HBA-pd) and poly(*m*HBA-pd)) shows approximately same activation energies (α = 0.6) and then the poly(*m*HBA-pd) shows a steep increase in the apparent activation energy. This may be attributed to the operation of different degradation mechanism leading to the formation different products. This is reflected in the TG curve of poly(*m*HBA-pd), which more complex compared to the TG curve of poly(*p*HBA-pd). Similar explanation is given by Lee et al [50] in estimation of cure and thermal degradation kinetics of epoxy organoclay nanocomposite. When the selected conversion became higher, the apparent activation energy increased, because as thermal degradation was proceeding, the molecules easily broken from the epoxy network were volatile at low temperature, however with the increasing degradation conversion, the stable residue that is present needs much higher temperature for further degradation. The average activation energy for the thermal degradation was 171 kJ/mol.

In the case of PQB, the apparent activation energy values vary from 252 to 330 kJ/mol (α= 0.1–0.9). Initially α value decreased upto the reaction extent level of 0.3. After reaction extent of 0.3, the Ea-D value increased steadily for higher values of α. The initial decrease in Ea-D values was attributed to the existence of weak points in the polymer chains whereas the higher Ea-D values at the later stages of degradation was associated with high degrees of random scission of the main chain. Krongauz [51] reported similar results for the crosslink density dependence of polymer degradation kinetics in photo crosslinked acrylates. The rotation of polymer segments is also consistent with low apparent activation energy of polyacrylate degradation and with an increase in activation energy with increase in crosslink density. Change from degradation due to rotation of polymer segments at low temperature to degradation through direct bond scission at higher temperatures may also explain increase in apparent activation energy with temperature.

Pitchaimari et al [52] reported similar results in studies on thermal degradation kinetics of thermal and UV cured N-(4-hydroxy phenyl) maleimide derivatives. The apparent activation energy values for the degradation of poly (N-(4-methacryloyloxyphenyl) maleimide (MAX) with N-vinyl-2-pyrrolidone (NVP)) as a comonomer (TDMAX) increased from 84 to 156 kJ/mol gradually with increasing extent of reaction (α= 0.1–0.9). The initial lower value of the apparent activation energy is most likely associated with the initiation process that occurs at these weak links. As these weak links are consumed, the limiting step of degradation shifts toward the degradation initiated by random scission, which typically has greater activation energy. The very high values of Ea-D calculated at large extents of degradation explain the large amount of solid residue remained. An increase of Ea-D with α has been also reported in literature for other types of polymers [53,54]. Achilias et al. [55] report similar result for the thermal degradation of light cured bisphenol-A glycidyldimethacrylate (Bis-GMA), bisphenol-A ethoxylated dimethacrylate (Bis-EMA), urethane dimethacrylate (UDMA) and triethylene glycol dimethacrylate (TEGDMA).

Initially for PRB, the apparent activation energy value increases with (Ea-D) increasing reaction extent values (α). After that the Ea-D values shows a continuous decrease for further reaction extent levels. This may be due to the difference in the structure of the net work formed and the way in which the degradation is initiated and propagated. Further as in the case of diamine based polybisbenzoxazines, in the diphenol based polybisbenzoxazines, the meta substituted system is showing much complexity compared to the para substituted system.

According to the statistical procedure proposed by Vyazovkin and Wight [8] the realistic confidence intervals for the activation energy determined are estimated for all the cases. The estimated activation energy and the Fisher confidence intervals for the three heating rates (10, 20, and 30 ºC/min) for the four samples are presented in Fig. 4.

Fig 4

3.4 TG-FTIR-Studies

The combination technique TG-FTIR provides information on neither the exact structure of all the decomposition products nor the separation of different decomposition products coming off at the same time. The thermal degradation processes of various polybenzoxazines were studied and the degradation mechanisms were proposed in the literature [21-24]. The structural effects of phenols and amines on the thermal degradation of polybenzoxazines were investigated systematically [56, 57].

The TG-FTIR studies of diphenol and diamine based polybisbenzoxazines have been carried out and the results are presented in Fig. 5 and 6 respectively.

Fig 5

Fig 6

The FTIR spectra shown in the Fig. 5 and 6 are for the mixture of products resulting from the thermal degradation of the chosen compounds.

The FTIR spectra of the volatiles formed from the polymers at the temperature where the rate of degradation is maximum are shown in Fig. 7.

Fig 7

The initial degradation for PQB starts around 200 °C and the degradation maximum was found to be at around 400 °C. In the initial stage of degradation, aromatic amine was the volatile product that has been released. Any two bond cleavages are sufficient to produce aromatic amines and N-alkyl substituted amines from PQB (Scheme 7). The cleavage of CH_2-N bond is necessary for the release of amines from degrading polybisbenzoxazines. The breakage of Ar-CH_2 bond is essential for the formation of substituted amines.

Scheme 7

The C–N bond dissociation energy (bond energy = 72 Kcal/mol) [58] is lower than the C–C bond dissociation energy (bond energy = 82.6 Kcal/mol). Hence it is reasonable to expect the initial degradation at the CH_2-N bond. A Schiff base (C=N) is formed when the Mannich base is cleaved. So, the next likely cleavage point is the C–C bond as the C–C bond (bond energy = 82.6 Kcal/mol) has a much lower bond energy than a C=N bond (bond energy = 147 Kcal/mol). In the bisphenol based polybisbenzoxazine structure, there are two equivalents C–N bonds that have equal probability of thermal cleavage. Aromatic amine is evolved as a degradation product which is favored at lower temperatures. A small absorption band observed at 3700 cm $^{-1}$ (Fig. 7) in the evolved gas proves in the initial stage of degradation proves the foregoing argument.

The degradation products of PQB and PRB are mainly various types of aromatic Schiff bases and substituted phenolic compounds, depending on the corresponding benzoxazine monomer structure. In addition, substituted benzene modes at1600, 1480, and 747 cm^{-1} were also detected in the FTIR spectra. These findings suggested that substituted phenols are the degradation products at this stage.

Formation of compounds having strong absorption band at 1670 cm^{-1} was detected at around 380 °C for PQB and PRB. This may be attributed to the evolution of Schiff bases from the degrading PQB and PRB. The possible degradation mechanism of this compound is shown in the Scheme 7.

The formation of phenols from PQB needs a minimum of four bond cleavages. At around 430 °C, a significant band at 3050 cm^{-1} was detected from degrading PQB (Fig. 7). This band is due to the free OH group of phenol and it is accompanied by a band at 1180 cm^{-1}, which is due to the C–O bond of phenol or substituted phenols. Hence the primary or the initial degradation of PQB and PRB is the formation of volatile aromatic amines followed by the evolution of phenolic compounds and this represents the temperature of the maximum rate of weight loss in the TG curves of both PRB and PQB. Thus, the degradation observed at higher temperatures in TG curves can be assigned to the evolution of phenolic compounds from the diphenol based polybisbenzoxazines.

Based on the TGA and FTIR evolved gas analyses (EGA), the thermal degradation mechanism of poly(*p*HBA-pd)have been proposed and is presented in Scheme 8.

Scheme 8

From the Fig. 7 one can conclude that aromatic amine and substituted aromatic amines were the major degradation products at the degradation stage where the rate degradation is found to be the maximum. The Schiff base was also detected as a degradation product from this polybisbenzoxazine at around 380 and 430 °C, for poly(*m*HBA-pd) and poly(*p*HBA-pd).The appearance of a band at 3650 cm^{-1} was significant. This is mainly attributed to the evolution of aromatic diamines. This temperature corresponds to the temperature of the maximum rate of weight loss in the TGA curves of poly(*p*HBA-pd) and poly(*m*HBA-pd).

4. Conclusion

It was found that the orientation of the polymerizable groups is having significant influence on the thermal degradation parameters. The material PQB (58%) shows relatively higher char value compared to materials poly(*m*HBA-pd) (34%), poly(*p*HBA-pd) (47%) and PRB(50%). The materials PQB and PRB show higher apparent activation energies for the thermal degradation process (Ea-D) (252 and 196 kJ/mol) when compared to poly(*p*HBA-pd) and poly(*m*HBA-pd) (98 and 95 kJ/mol) at the initial degradation stage. Aromatic amines are found to be released in considerable quantities from the diamine based polybisbenzoxazines whereas phenolic compounds are released from diphenol based polybisbenzoxazines. The thermal stability and the products formed during the thermal degradation may be explained on the basis of the inter and intamolecular hydrogen bonded structures resulting from the thermal polymerization of the bisbenzoxazine monomers.

5. Acknowledgement

Sincere thanks are due to the Management and the Principal of Kamaraj College of Engineering and Technology, S. P. G. C. Nagar, K. Vellakulam - 625 701 for their constant encouragement and support

Reference

1. A. Gardziella, L. A. Pilato, A. Knop, Phenolic Resins: Chemistry, Applications, Standardisation, Safety, and Ecology, Springer- Verlag, Heidelberg, Germany, 2000.
2. F. W. Holly, A. C. Cope, Condensation product of aldehydes and ketones with o-aminobenzyl alcohol and o-hydroxybenzylamine, J. Am. Chem. Soc. 66 (1944) 1875-1879.
3. Y. Liu, Z. Yue, Z. Li, Z. Liu, Thermal degradation behavior and kinetics of polybenzoxazine based on bisphenol-S and aniline Thermochim Acta, 523 (2011), 523 (1-2), 170-175.
4. C. Jubsilp, S. Damrongsakkul, T. Takeichi, S. Rimdusit, Curing kinetics of arylamine-based polyfunctional benzoxazine resins by dynamic differential scanning calorimetry, Thermochim Acta, 477 (2006) 131-140.
5. S. Montserrat, J. Malek, A kinetics analysis of the curing reaction of an epoxy resin, Thermochim Acta, 228 (1993) 47-60.
6. G. Reiss, J. M. Schwob, G. Guth, M. Roche, B. Lande, Advances in Polymer Synthesis, ed. by Culbertson, B.M. and McGrath, J.E., Plenum, New York, (1985), 27.
7. S. Shamim Rishwana, G. Pitchaimari, C. T. Vijayakumar, Studies on structurally different benzoxazines based on diphenols and diamines:

synthesis and kinetics of thermal curing, High. Perform. Polym, (2015) Accepted (DOI: 10.1177/0954008315587125)

8. S. Vyazovkin, C.A. Wight, Estimating realistic confidence intervals for the activation energy determined from thermoanalytical measurements, Anal. Chem. 72 (2000) 3171–3175.
9. S. Vyazovkin, C.A. Wight, Isothermal and non-isothermal kinetics of thermally stimulated reactions of solids, Int. Rev. Phys. Chem. 17 (3) (1998) 407–433.
10. S. Vyazovkin, N. Sbirrazzuoli, Mechanism and kinetics of epoxy-amine cure studied by differential scanning calorimetry. Macromolecules 11 (1996) 1867-1873.
11. S. Vyazovkin, Computational aspects of kinetic analysis.: Part C. The ICTAC Kinetics Project - the light at the end of the tunnel?, Thermochim. Acta. 355 (1999) 155-163.
12. S. Vyazovkin, A unified approach to kinetic processing of nonisothermal data, Int. J. Chem. Kinet. 28 (1996) 95-101.
13. S. Vyazovkin, A. K. Burnham, J. M. Criado, L. A. Perez-Maqueda, C. Popescu, N. Sbirrazzuoli, ICTAC Kinetics Committee recommendations for performing kinetic computations on thermal analysis data, Thermochim. Acta. 520 (2011) 1–19.

14. H. L. Friedman, Kinetics of thermal degradation of char-forming plastics from thermogravimetry. Application to a phenolic plastic. J polym sci, part C: polym sym 64 (1964) 183-195.
15. H. E. Kissinger, Reaction kinetics in differential thermal analysis. Anal chem 11 (1957) 1702-1706.
16. A. W. Coats, J. P. Redfern, Kinetic parameters from thermogravimetric data. Nature 201 (1964) 68-69.
17. C .A Wilkie, TGA/FTIR: an extremely useful technique for studying polymer degradation, Polym. Degrad. Stabil. 66 (1999) 301-306.
18. F. Hoffmann, R. Riesen, J. Foreman, Characterization of thermal stability and reaction products by means of TGA-FTIR coupling, J., Am. Lab. 32 (2000) 13.
19. K. G. H. Raemaekers, J. C. J. Bart, Applications of simultaneous thermogravimetry- mass spectrometry in polymer analysis Thermochim. Acta, 29(1997) 1-58.
20. K. L. Sobeih, M. Baron, J. Gonzalez-Rodriguez, Recent trends and developments in pyrolysis-gas chromatography, J. Chromatog. A, 1186 (2008) 51-66.

21. H. Y. Low, H. Ishida, Mechanistic study on the thermal decomposition of polybenzoxazines: effects of aliphatic amines, J. Polym. Sci. B Polym. Phys 36 (1998) 1935-1946.
22. H. Y. Low, H. Ishida, Structural effects of phenols on the thermal and thermo-oxidative degradation of polybenzoxazines Polymer, 40 (1999) 4365-4376.
23. H. Y. Low, H. Ishida, An investigation of the thermal and thermooxidative degradation of polybenzoxazines with a reactive functional group, J. Polym. Sci. B Polym. Phys, 37 (1999) 647-659.
24. Z. Brunovska, H. Ishida, Thermal study on the copolymers of phthalonitrile and phenylnitrile-functional benzoxazines, J. Appl. Polym. Sci. 73 (1999) 2937-2949.
25. H.J. Kim, Z. Brunovska, H. Ishida, Synthesis and thermal characterization of polybenzoxazines based on acetylene-functional monomers, Polymer 40 (1999) 6565–6573.
26. C. T. Vijayakumar, S. Shamim Rishwana, R. Surender, N. David Mathan, S. Vinayagamoorthi, S. Alam, Structurally diverse benzoxazines: synthesis, polymerization, and thermal stability, Des Monomers Polym, 17 (2014) 17: 47.

27. S. Shamim Rishwana, A. Mahendran, C. T. Vijayakumar, Studies on structuraly different benzoxazines: curing characteristics and thermal degradation aspects High perform Polym Epub ahead of print 11 December 2014. DOI: 10.1177/0954008314561806.
28. C. H. Lin, Y. R. Taso, J. W. Sie, H. H. Lee, Processes of synthesis of aromatic amine-based benzoxazine resins, 2010, U.S. Pat., 7,781,561.
29. B. Kiskan, B. Aydogan, Y. Yagci, Synthesis, Characterization, and Thermally Activated Curing of Oligosiloxanes Containing Benzoxazine Moieties in the Main Chain, J polym sci, part A: polym chem. 47 (2009) 804-811.
30. B. Jankovic, B. Adnadevic, J. Jovanovic, Application of model-fitting and-free kinetics to the study of non-isothermal dehydration of equilibrium swollen poly (acrylic acid) hydrogel, Thermochim Acta 452 (2007) 106-115.
31. D. R. Yei, H. K. Fu, W. Y. Chen, Synthesis of a novel benzoxazine monomer-intercalated montmorillonite and the curing kinetics of polybenzoxazine/clay hybrid nanocomposites. J Polym Sci Pol Phy 44 (2006) 347-358.

32. P. Budrugeac, E. Segal, Some methodological problems concerning nonisothermal kinetic analysis of heterogeneous solid–gas reactions. Int J Chem Kinet 33 (2001) 564-573.
33. C. D. Doyle, Estimating isothermal life from thermogravimetric data. J Appl Polym Sci 6 (1962) 639-642.
34. V. M. Gorbachev, A solution of the exponential integral in the non-isothermal kinetics for linear heating. J Therm Analy Calorim 8 (1975) 349-350.
35. R. K. Agarwal, M. S. Sivasubramanian, International approximations for nonisothermal kinetics. AIChe J 32 (1987) 1212-1214.
36. J. Cai, F. Yao, W. Yi, F. HE, New temperature integral approximation for nonisothermal kinetics. AIChe J 52 (2006) 1554-1557.
37. S. Vyazovkin, D. Dollimore, Linear and non-linear procedures in isoconversional computations of the activation energy of nonisothermal reactions in solids. J Chem Inf Comp Sci 36 (1996) 42-45.
38. A. Kandelbauer, G. Wuzella, A. Mahendran, I. Taudes, P. Widsten, Using isoconversional kinetics analysis of liquid melamine-formaldehyde resin curing to predict laminate surface properties. J Appl Polym Sci 113 (2009) 2649-2660.

39. H. Ishida, T. Agag, Hand book of benzoxazine resins. Elsevier's publication 2011.

40. T. Agag, T. Takeichi, Novel benzoxazine monomers containing p-phenyl propargylether: polymerization of monomers and properties of polybenzoxazines, Macromolecules 34 (2001) 7257-7263.

41. T. Agag, T. Takeichi, Synthesis and characterization of novel benzoxazine monomers containing allyl groups and their high performance thermosets. Macromolecules 36 (2003) 6010-6017.

42. Z. Brunovska, J. P. Liu, H. Ishida, 1,3,5-Triphenylhexahydro-1,3,5-triazine active intermediate and precursor in the novel synthesis of benzoxazine monomers and oligomers. Macromol Chem Phy. 200 (1999) 1745-1752.

43. H. Kimura, A. Matsumoto, K. Hasegawa, K. Ohtsuka, A. Fukuda, Epoxy resin cured by bisphenol A based benzoxazine J Appl Polym Sci 68 (1998) 1903-1910.

44. H. Ishida, K. Hemvichian, Thermal decomposition processes in aromatic amine-based polybenzoxazines investigated by TGA and GC–MS, Polymer 43 (2002) 4391-4402.

45. H. Y. Low, H. Ishida, Structural effects of phenols on the thermal and thermo-oxidative degradation of polybenzoxazines, Polymer (1999) 4365-4402.

46. H. J. Kim, Z. Brunovska, H. Ishida, Molecular characterization of the polymerization of acetylene-functional benzoxazine resins, Polymer 40 (1999) 1815-1822.

47. H. J. Kim, Z. Brunovska, H. Ishida, Synthesis and thermal characterization of polybenzoxazines based on acetylene-functional monomers , Polymer 40 (1999) 6565-6573.

48. T. Agag, T. Takeichi, Novel Benzoxazine Monomers Containing *p*-Phenyl Propargyl Ether: Polymerization of Monomers and Properties of Polybenzoxazines, Macromolecules 34 (2001) 7257-7263.

49. Z. Brunovska, H. Ishida, Thermal study on the copolymers of phthalonitrile and phenylnitrile-functional benzoxazines, J Appl Polym Sci 73 (1999) 2937-2949.

50. J. Lee. B. Choi, H. Lee, Estimation of cure and thermal degradation kinetics of epoxy/organoclay nanocomposite, Advanced Materials Research, 123-125 (2010) 667-670.

51. V. V. Krongauz, Crosslink density dependence of polymer degradation kinetics:photocrosslinked acrylates Thermochim. Acta 503 (2010) 70-84.

52. G. Pitchaimari, C. T. Vijayakumar, Studies on thermal degradation kinetics of thermal and UV curedN-(4-hydroxy phenyl) maleimide derivatives, Thermochim Acta, 575 (2014) 70-80.

53. J. D. Peterson, S. Vyazovkin, C. A. Wight, Kinetics of the thermal and thermo-oxidative degradation of polystyrene, polyethylene and polypropylene Macromol. Chem. Phys. 202 (2001) 775-784.

54. K. Chrissafis, K.M. Paraskevopoulos, D.N. Bikiaris, Effect of molecular weight onthermal degradation mechanism of the biodegradable polyester poly(ethylenesuccinate), Thermochim. Acta 440 (2006) 166–175.

55. D.S. Achilias, M.M. Karabela, I.D. Sideridou, Thermal degradation of light-cureddimethacrylate resins Part I. Isoconversional kinetic analysis, Thermochim.Acta 472 (2008) 74–83.

56. H. Ishida, D.P. Sanders, Improved thermal and mechanical properties of polybenzoxazines based on alkyl-substituted aromatic amines, J. Polym. Sci. B Polym. Phys. 38 (2000) 3289–3301.

57. K. Hemvichian, H.D. Kim, H. Ishida, Identification of volatile products and determination of thermal degradation mechanisms of polybenzoxazine model oligomers by GC-MS, Polym. Degrad. Stabil. 87 (2005) 213–224.

58. Pauling, L., Chemical Bonds, in: Cornell University Press, New York, 1960, p. 85

Legend to Figures

Fig. 1 FTIR of the bisbenzoxazine monomers and their polymers

Fig. 2 The TG and DTG traces for poly(*p*HBA-pd), poly(*m*HBA-pd), PQB and PRB recorded at multiple heating rates (10, 20and 30°C/min)

Fig. 3 Relative reaction extent vs apparent activation energies of polybisbenzoxazines

Fig. 4 Activation energy and Fisher confidence intervals for the polymerized compound at heating rate (10, 20and 30°C/min) estimates (Vyazovkin method).

Fig. 5 The TG, DTG and TG-FTIR curves of PQB and PRB at 10 ºC/min.

Fig. 6 The TG, DTG and TG-FTIR curves of poly(*p*HBA-pd) and poly(*m*HBA-pd) at 10 ºC/min.

Fig. 7 FTIR spectra of the volatiles formed from the polymers at the temperature where the rate of degradation is maximum.

Legend to Scheme

Scheme 1 Preparation of *p*-phenylenediaminebisbenzoxazine (*p*HBA-pd) and *m*-phenylenediaminebisbenzoxazine

Scheme 2 Preparation of quinolbisbenzoxazine (QB) and resorcinolbisbenzoxazine (RB).

Scheme 3 The proposed polymeric structure of PQB and intermolecular hydrogen bonding

Scheme 4 The proposed polymeric structure of PRB and intramolecular hydrogen bonding

Scheme 5 The proposed polymeric structure of poly(*p*HBA-pd) and intermolecular hydrogen bonding

Scheme 6 The proposed polymeric structure of poly(*m*HBA-pd) and intramolecular hydrogen bonding

Scheme 7 The possible degradation mechanism of PQB

Scheme 8 Proposed mechanism for the thermal degradation of poly(*p*HBA-pd).

Table Captions

Table 1 The full names and abbreviated names of the materials

Table 2 TG studies: The degradation parameters for the different polybisbenzoxazines recorded at 10 °C/min

Table 1 The full names and abbreviated names of the materials

Name	Abbreviated name
Resorcinolbisbenzoxazine	RB
Quinolbisbenzoxazine	QB
m-Phenylenediaminebisbenzoxazine	*m*HBA-pd
p-Phenylenediaminebisbenzoxazine	*p*HBA-pd
Polyresorcinolbisbenzoxazine	PRB
Polyquinolbisbenzoxazine	PQB
Poly*m*-phenylenediaminebisbenzoxazine	poly(*m*HBA-pd)
Poly*p*-phenylenediaminebisbenzoxazine	poly(*p*HBA-pd)

Table 2 TG studies: The degradation parameters for the different polybisbenzoxazines recorded at 10 °C/min

Sample	Temperature(°C)					T_{Max}(°C)			Char yield % at 800°C
	T_5	T_{10}	T_{25}	T_i	T_e	T_{M1}	T_{M2}	T_{M3}	
PRB	270	318	431	254	569	310	330	430	50
PQB	289	354	501	268	539	-	380	-	58
poly(*m*HBA-pd)	214	243	307	231	570	274	380	530	34
poly(*p*HBA-pd)	369	410	470	331	544	-	430	-	47

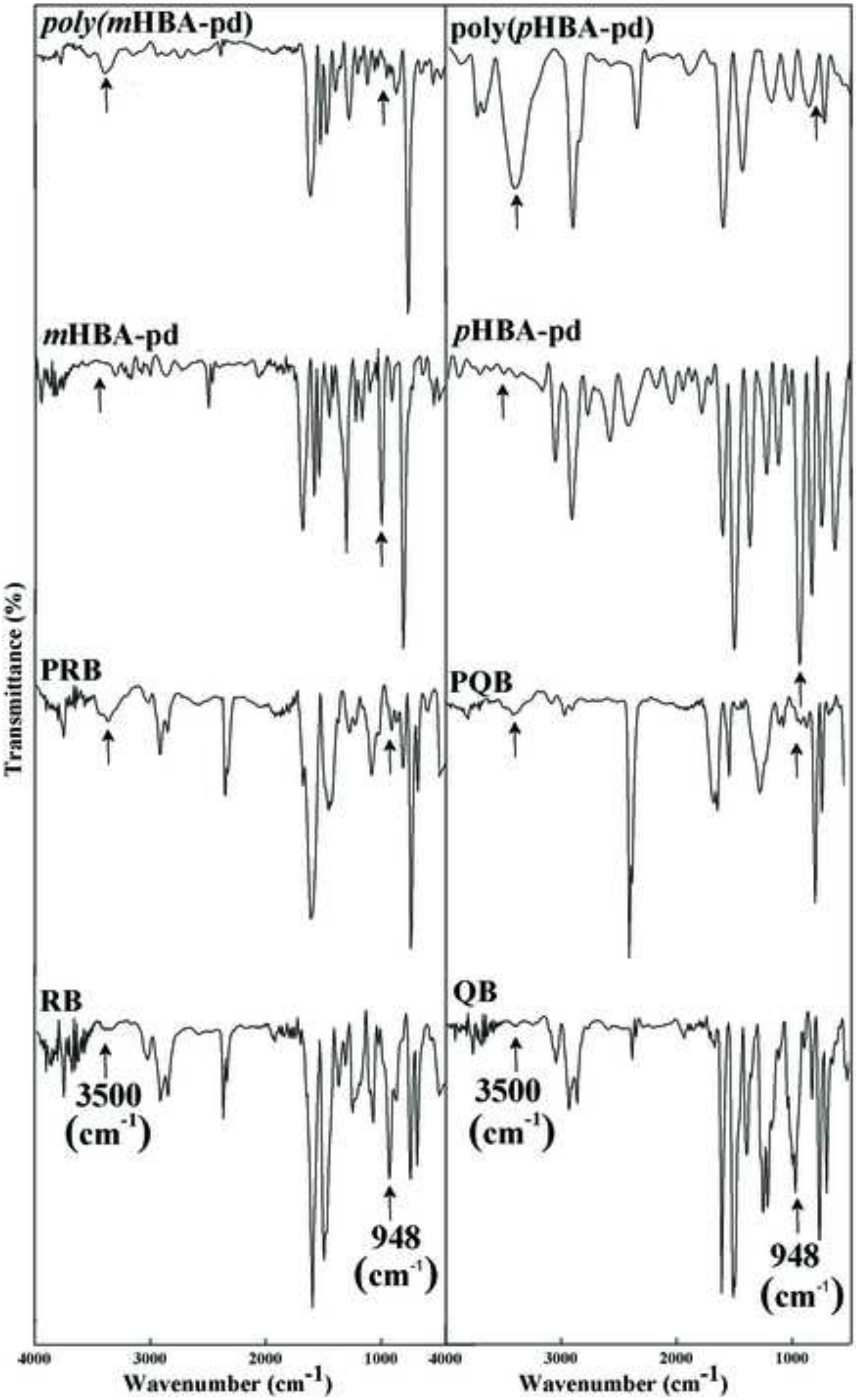
poly(mHBA-pd)
poly(pHBA-pd)
mHBA-pd
pHBA-pd
PRB
PQB
RB
QB
3500 (cm-1)
3500 (cm-1)
948 (cm-1)
948 (cm-1)
Transmittance (%)
4000
3000
2000
1000
4000
3000
2000
1000
Wavenumber (cm-1)
Wavenumber (cm-1)

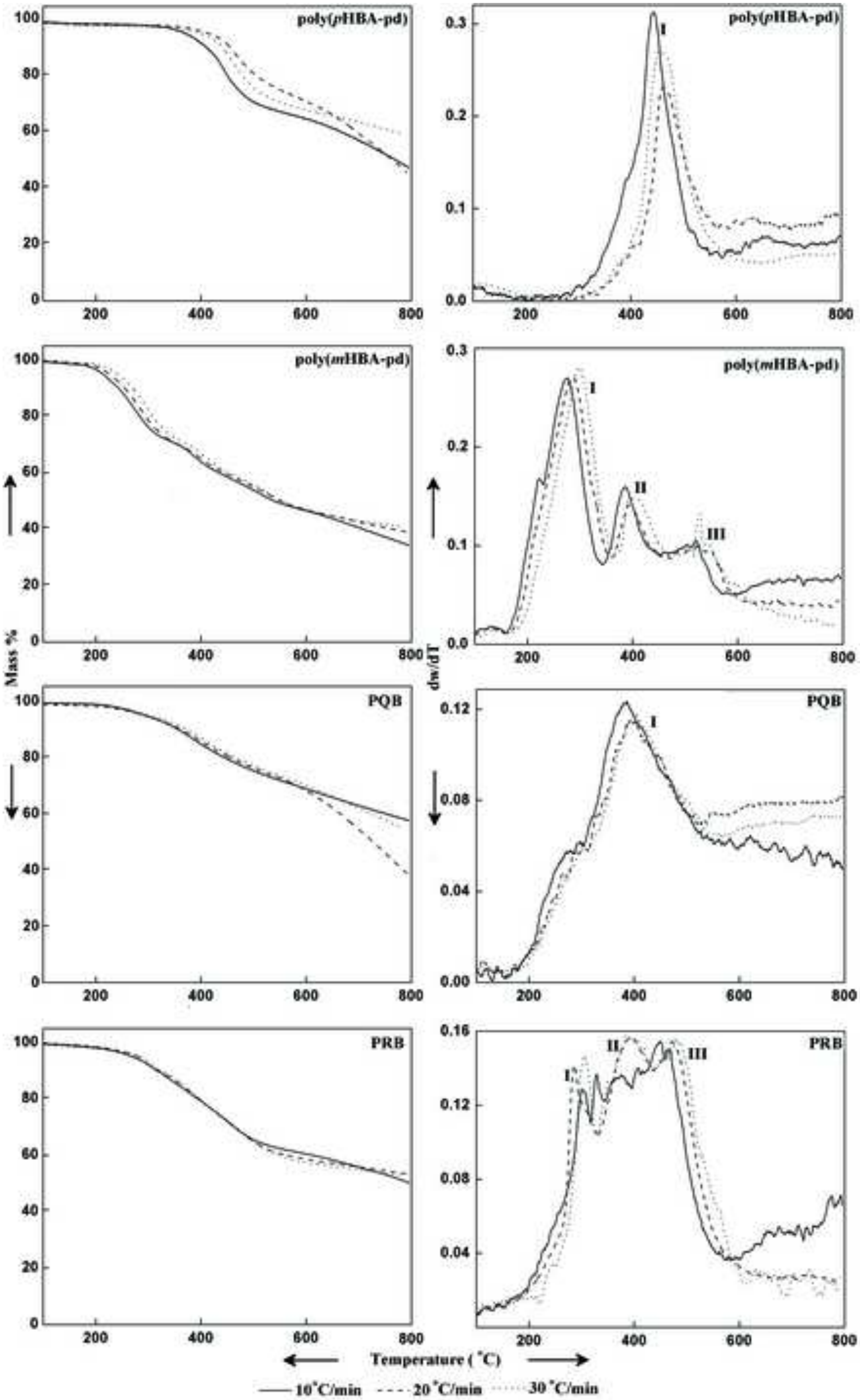
poly(pHBA-pd)
I
poly(mHBA-pd)
I
II
III
PQB
I
PRB
I
II
III
Mass %
dw/dT
0
20
40
60
80
100
0.0
0.1
0.2
0.3
0.00
0.04
0.08
0.12
0.16
200
400
600
800
Temperature (°C)
10°C/min
20°C/min
30°C/min

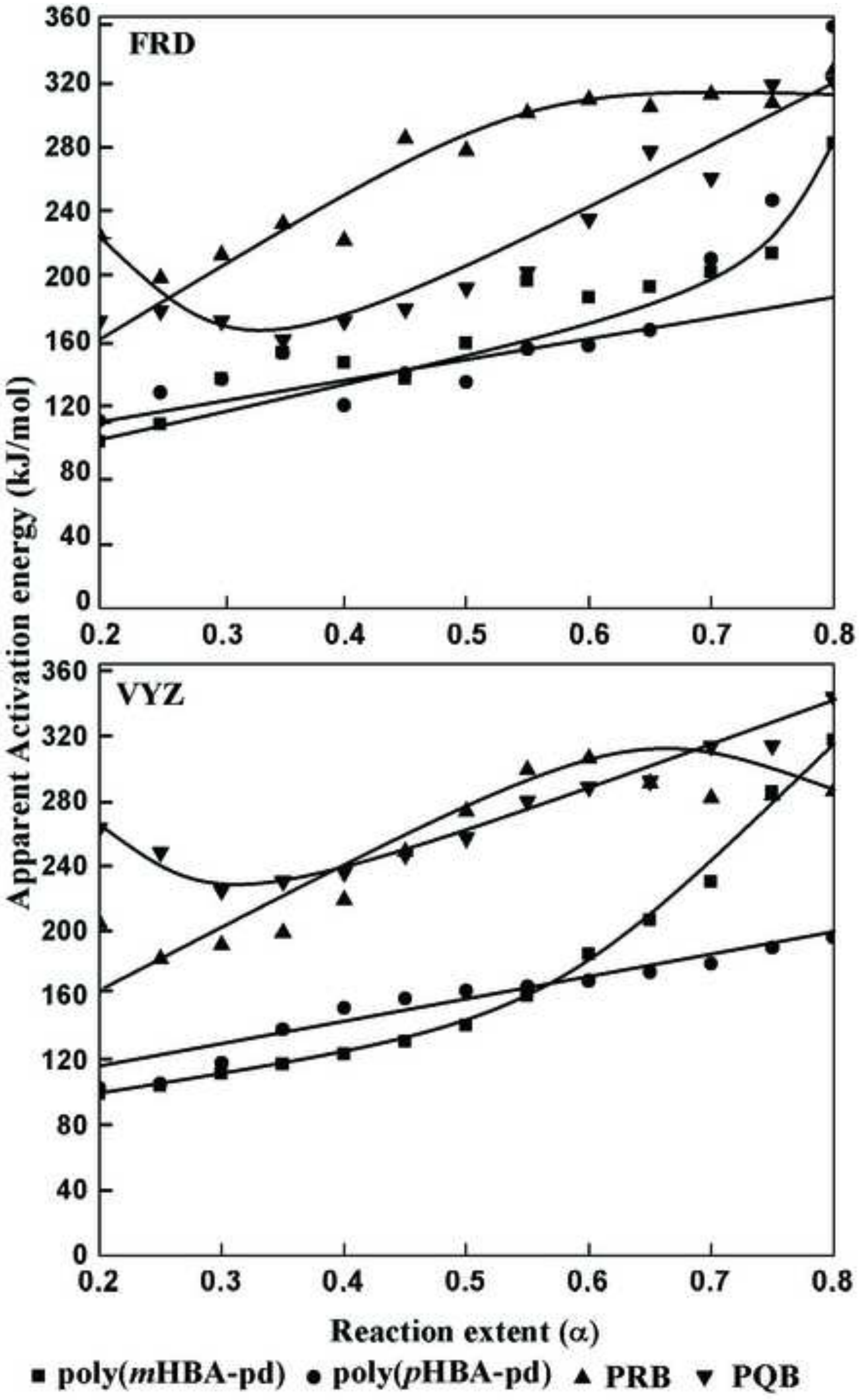
FRD
VYZ
360
320
280
240
200
160
120
80
40
0
0.2
0.3
0.4
0.5
0.6
0.7
0.8
Apparent Activation energy (kJ/mol)
Reaction extent (α)
■ poly(*m*HBA-pd) ● poly(*p*HBA-pd) ▲ PRB ▼ PQB

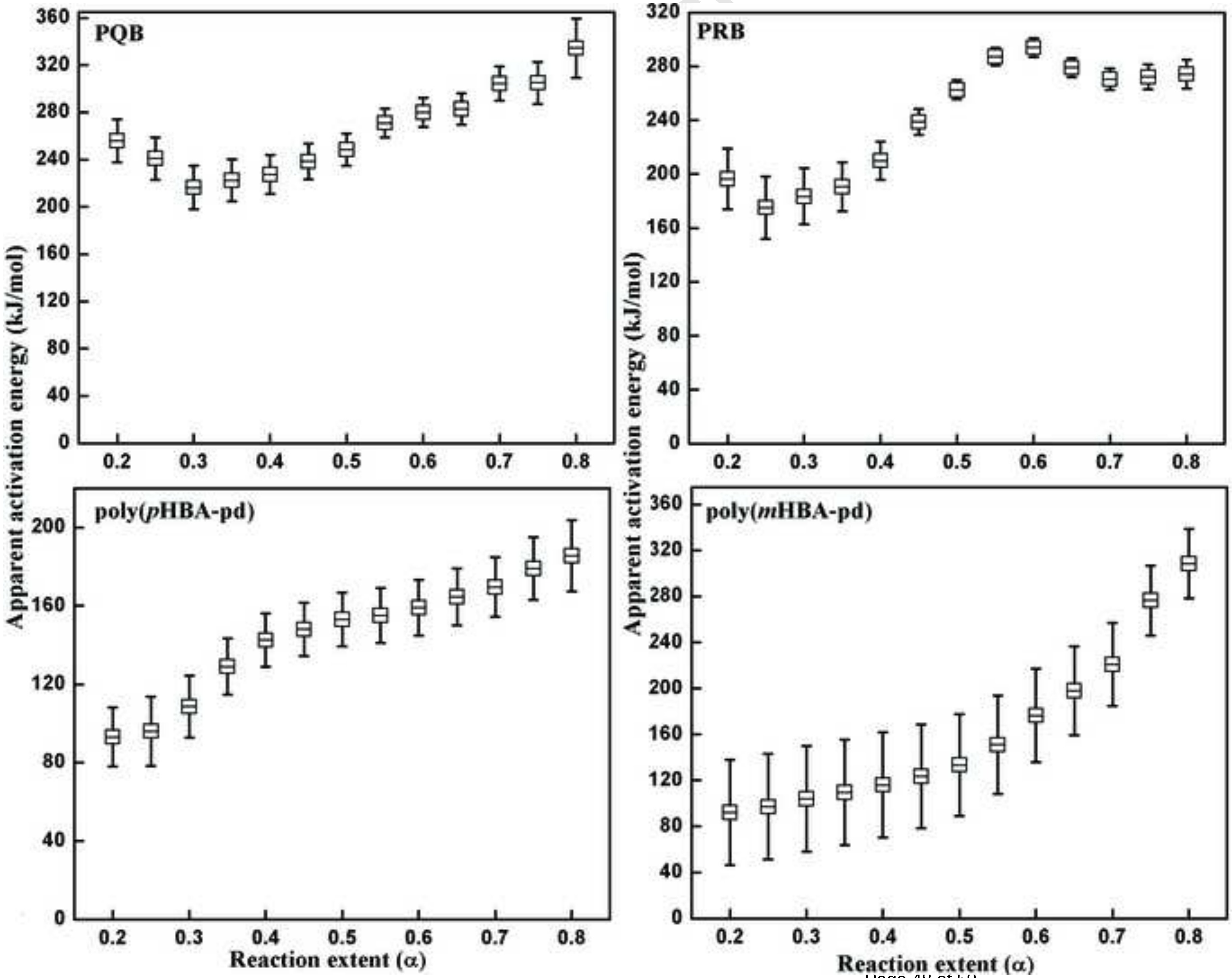
PQB
PRB
poly(*p*HBA-pd)
poly(*m*HBA-pd)
Apparent activation energy (kJ/mol)
Apparent activation energy (kJ/mol)
Reaction extent (α)
Reaction extent (α)
0
40
80
120
160
200
240
280
320
360
0.2
0.3
0.4
0.5
0.6
0.7
0.8

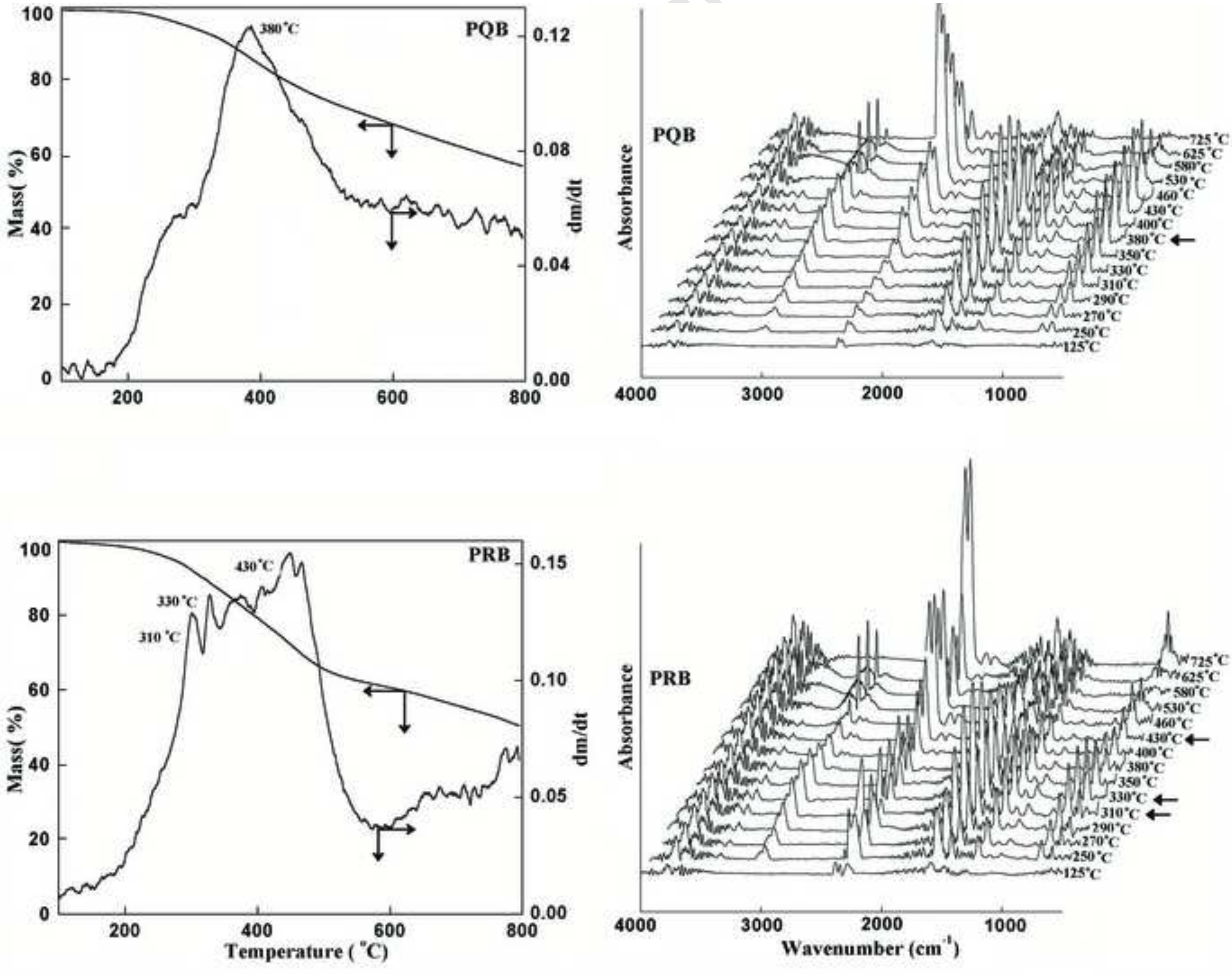
PQB
380°C
Mass(%)
dm/dt
100
80
60
40
20
0
0.12
0.08
0.04
0.00
200
400
600
800
Absorbance
PQB
725°C
625°C
580°C
530°C
460°C
430°C
400°C
380°C
350°C
330°C
310°C
290°C
270°C
250°C
125°C
4000
3000
2000
1000
PRB
430°C
330°C
310°C
Mass(%)
dm/dt
0.15
0.10
0.05
0.00
Temperature (°C)
Absorbance
PRB
725°C
625°C
580°C
530°C
460°C
430°C
400°C
380°C
350°C
330°C
310°C
290°C
270°C
250°C
125°C
Wavenumber (cm⁻¹)

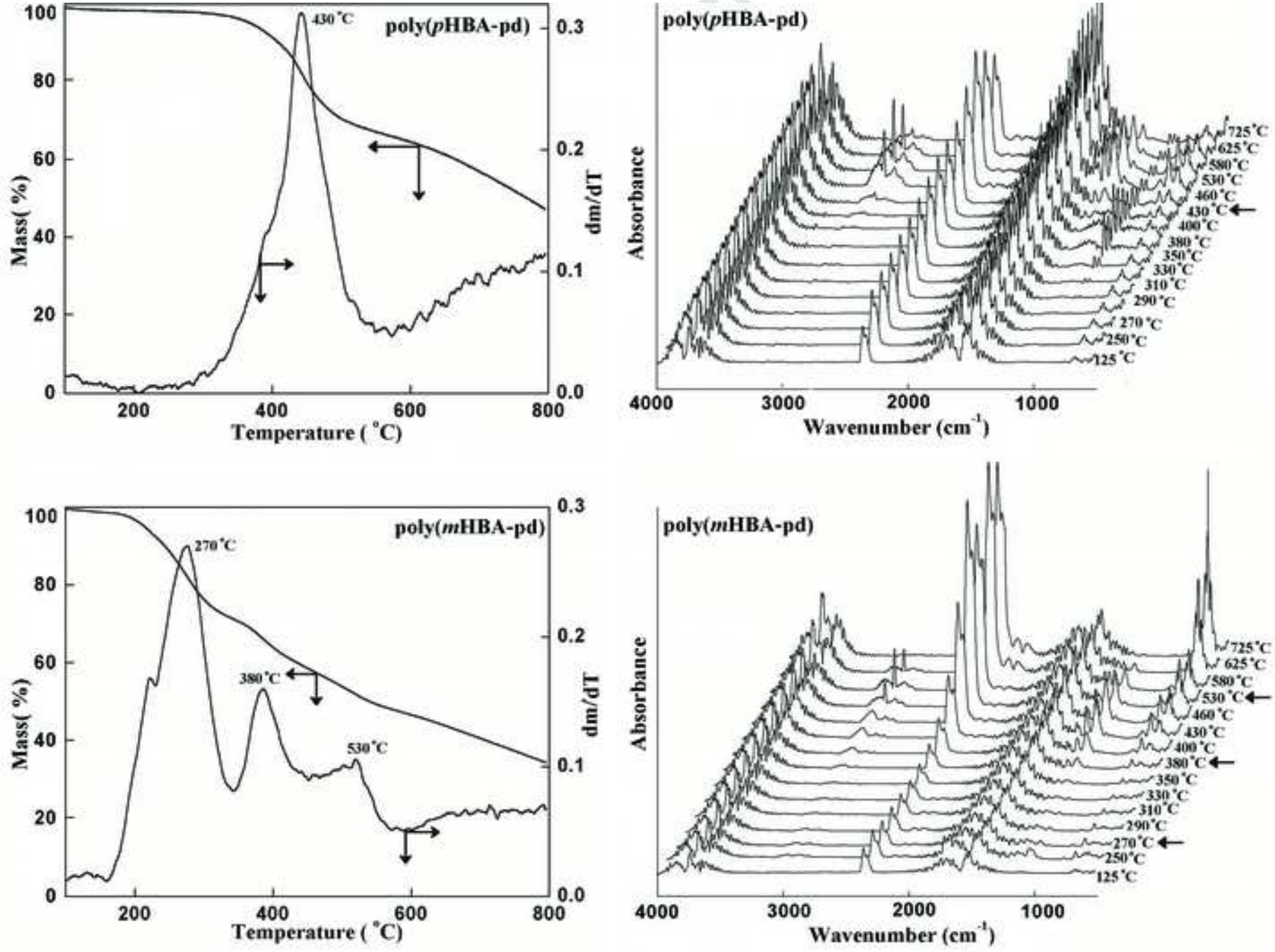
poly(pHBA-pd)
430 °C
Mass(%)
100
80
60
40
20
0
dm/dT
0.3
0.2
0.1
0.0
200
400
600
800
Temperature (°C)
poly(pHBA-pd)
Absorbance
725 °C
625 °C
580 °C
530 °C
460 °C
430 °C
400 °C
380 °C
350 °C
330 °C
310 °C
290 °C
270 °C
250 °C
125 °C
4000
3000
2000
1000
Wavenumber (cm-1)
poly(mHBA-pd)
270 °C
380 °C
530 °C
Mass(%)
100
80
60
40
20
0
dm/dT
0.3
0.2
0.1
0.0
200
400
600
800
Temperature (°C)
poly(mHBA-pd)
Absorbance
725 °C
625 °C
580 °C
530 °C
460 °C
430 °C
400 °C
380 °C
350 °C
330 °C
310 °C
290 °C
270 °C
250 °C
125 °C
4000
3000
2000
1000
Wavenumber (cm-1)

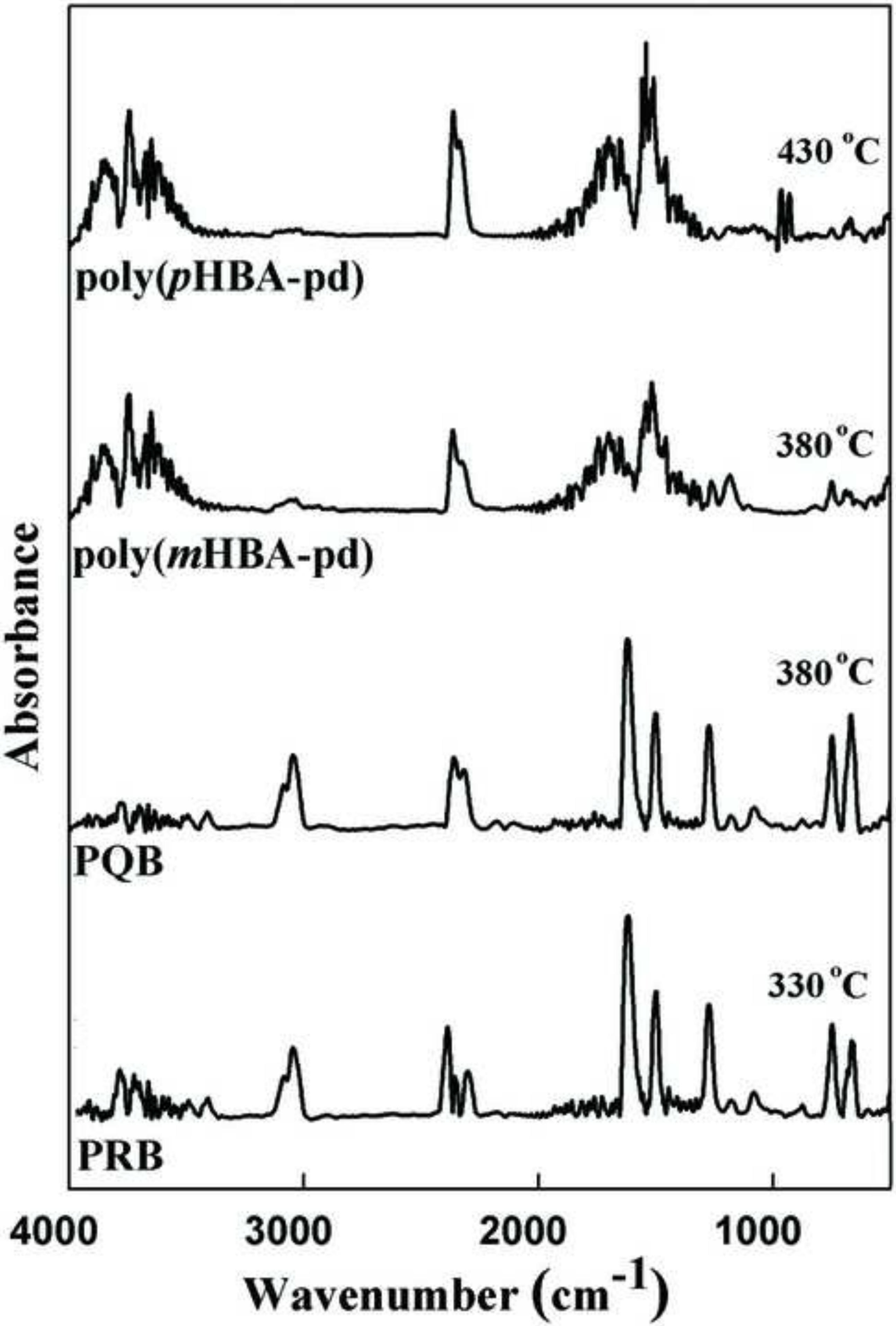
430 °C
poly(*p*HBA-pd)
380 °C
poly(*m*HBA-pd)
380 °C
PQB
330 °C
PRB
Absorbance
4000
3000
2000
1000
Wavenumber (cm^{-1})

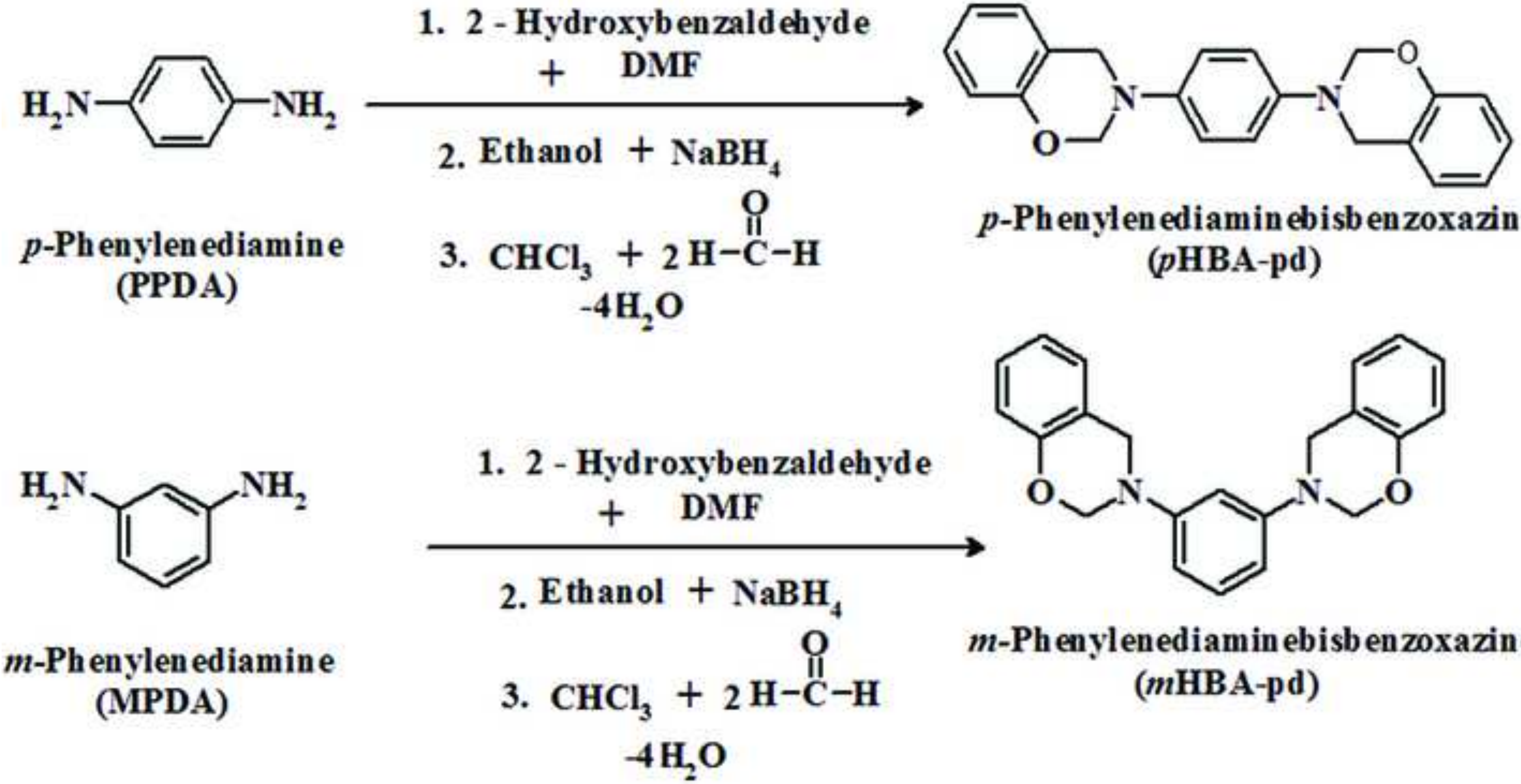
H₂N
NH₂
p-Phenylenediamine
(PPDA)
1. 2 - Hydroxybenzaldehyde
+ DMF
2. Ethanol + NaBH₄
3. CHCl₃ + 2 H−C(=O)−H
-4H₂O
N
O
N
O
p-Phenylenediaminebisbenzoxazine
(pHBA-pd)
H₂N
NH₂
m-Phenylenediamine
(MPDA)
1. 2 - Hydroxybenzaldehyde
+ DMF
2. Ethanol + NaBH₄
3. CHCl₃ + 2 H−C(=O)−H
-4H₂O
O
N
N
O
m-Phenylenediaminebisbenzoxazine
(mHBA-pd)

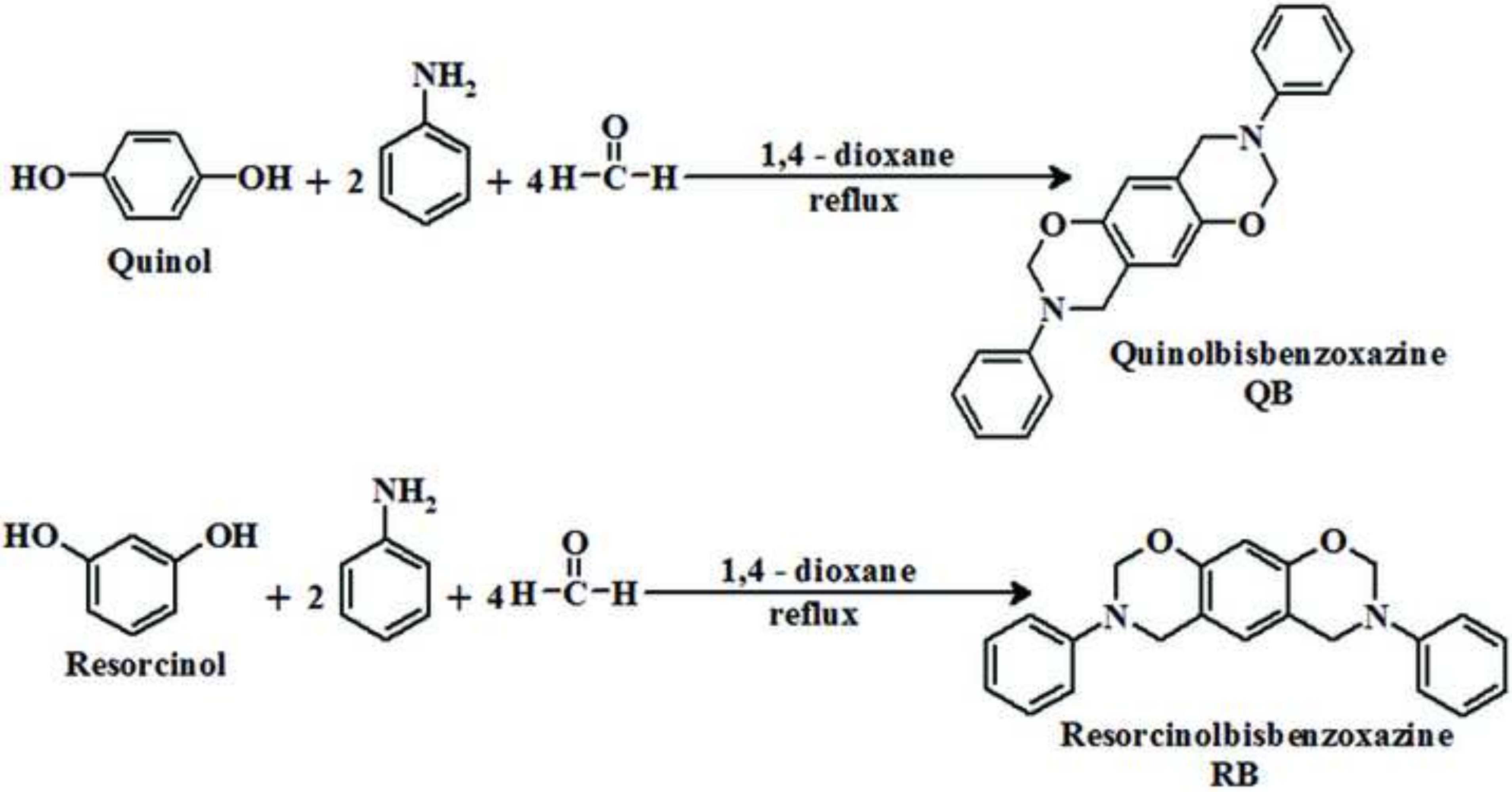
HO
OH
+ 2
NH_2
+ 4 H–C(=O)–H
1,4 - dioxane
reflux
Quinol
O
N
Quinolbisbenzoxazine
QB
HO
OH
+ 2
NH_2
+ 4 H–C(=O)–H
1,4 - dioxane
reflux
Resorcinol
O
N
Resorcinolbisbenzoxazine
RB

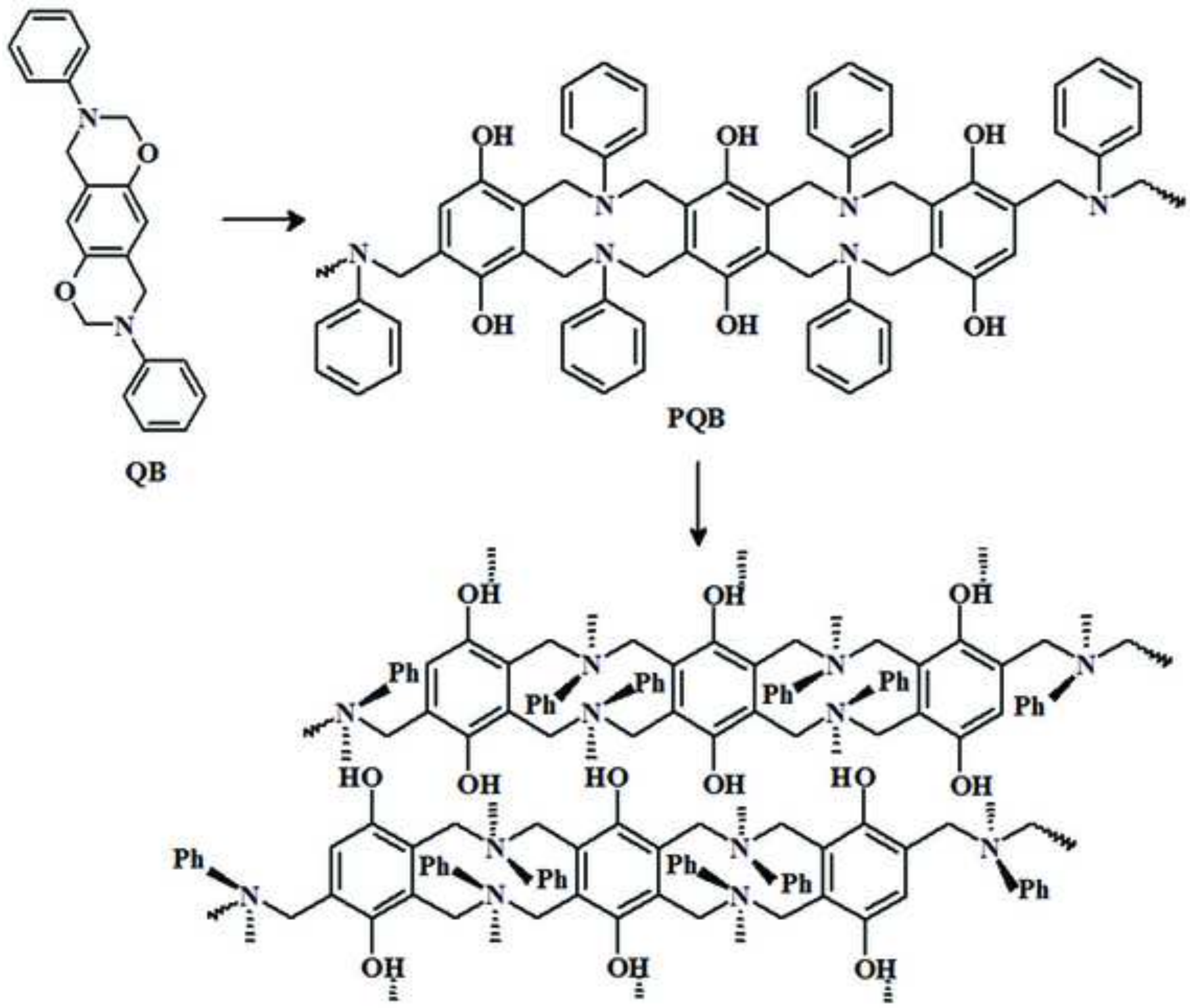

QB

PQB

PQB

Intermolecular hydrogen bonding

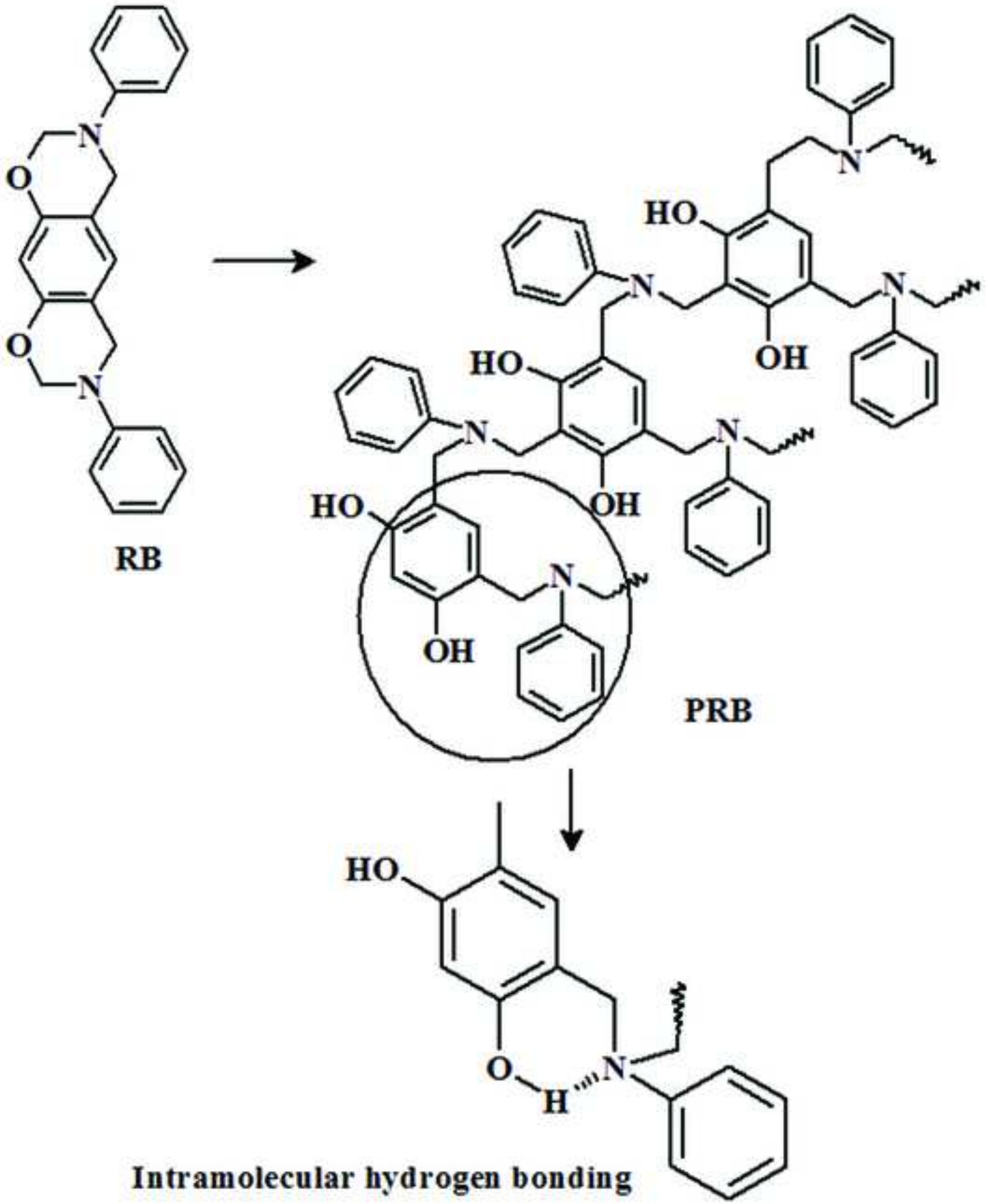
O
N
O
N
RB
HO
N
OH
HO
N
OH
HO
N
OH
N
N
N
PRB
HO
O
H
N
Intramolecular hydrogen bonding

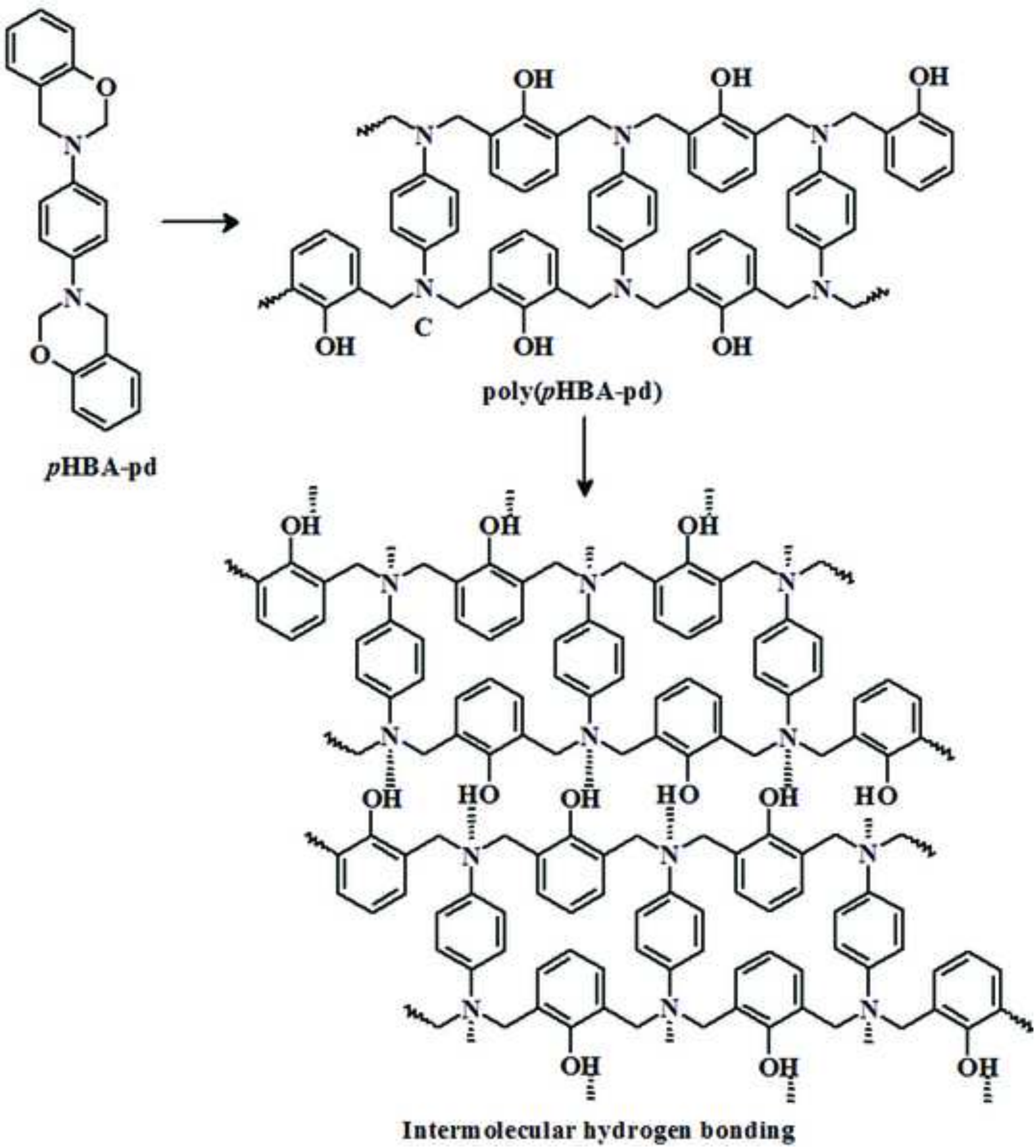
O
N
N
O
*p*HBA-pd
OH
N
C
poly(*p*HBA-pd)
HO
Intermolecular hydrogen bonding

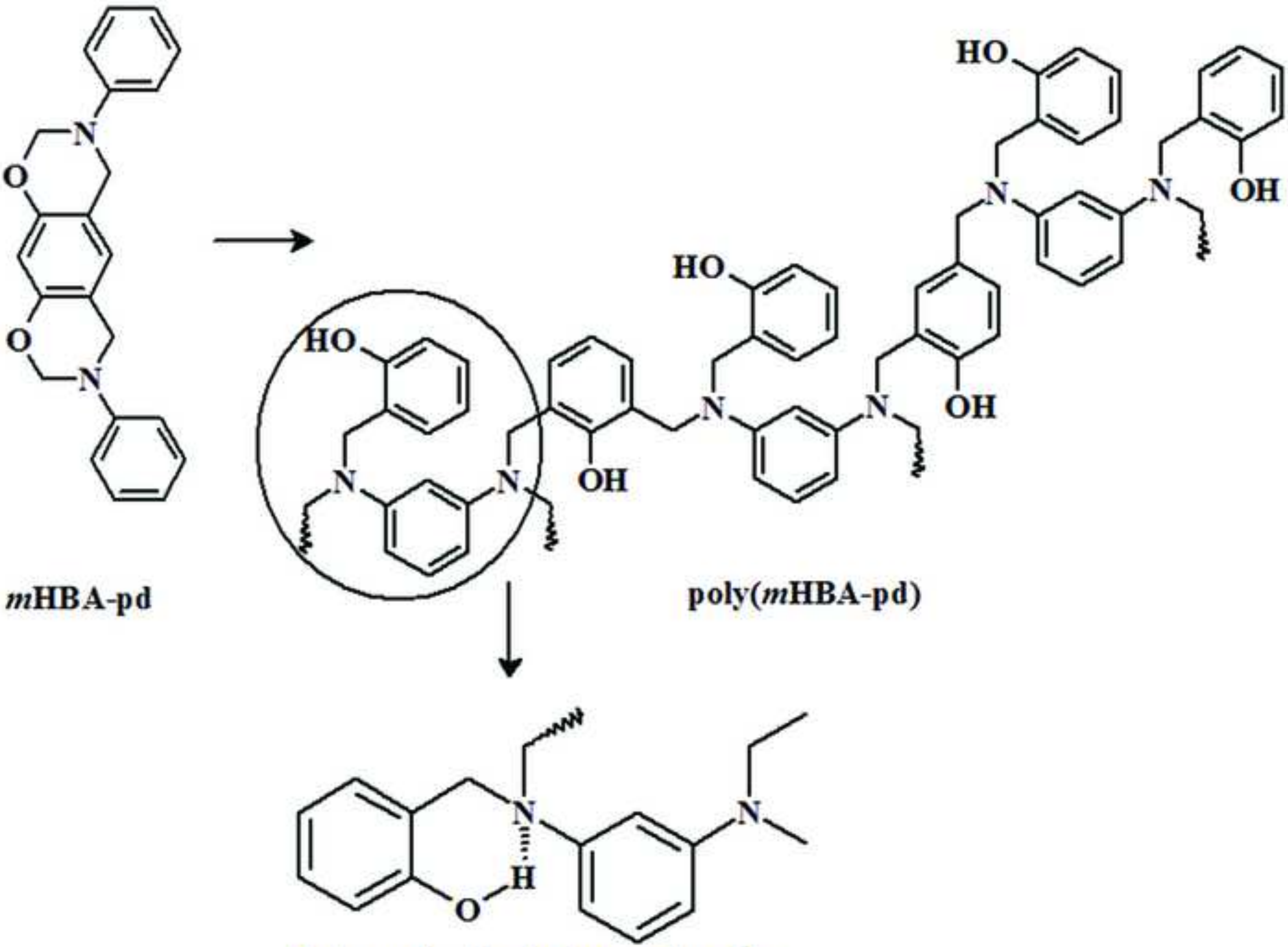

*m*HBA-pd

poly(*m*HBA-pd)

Intramolecular hydrogen bonding

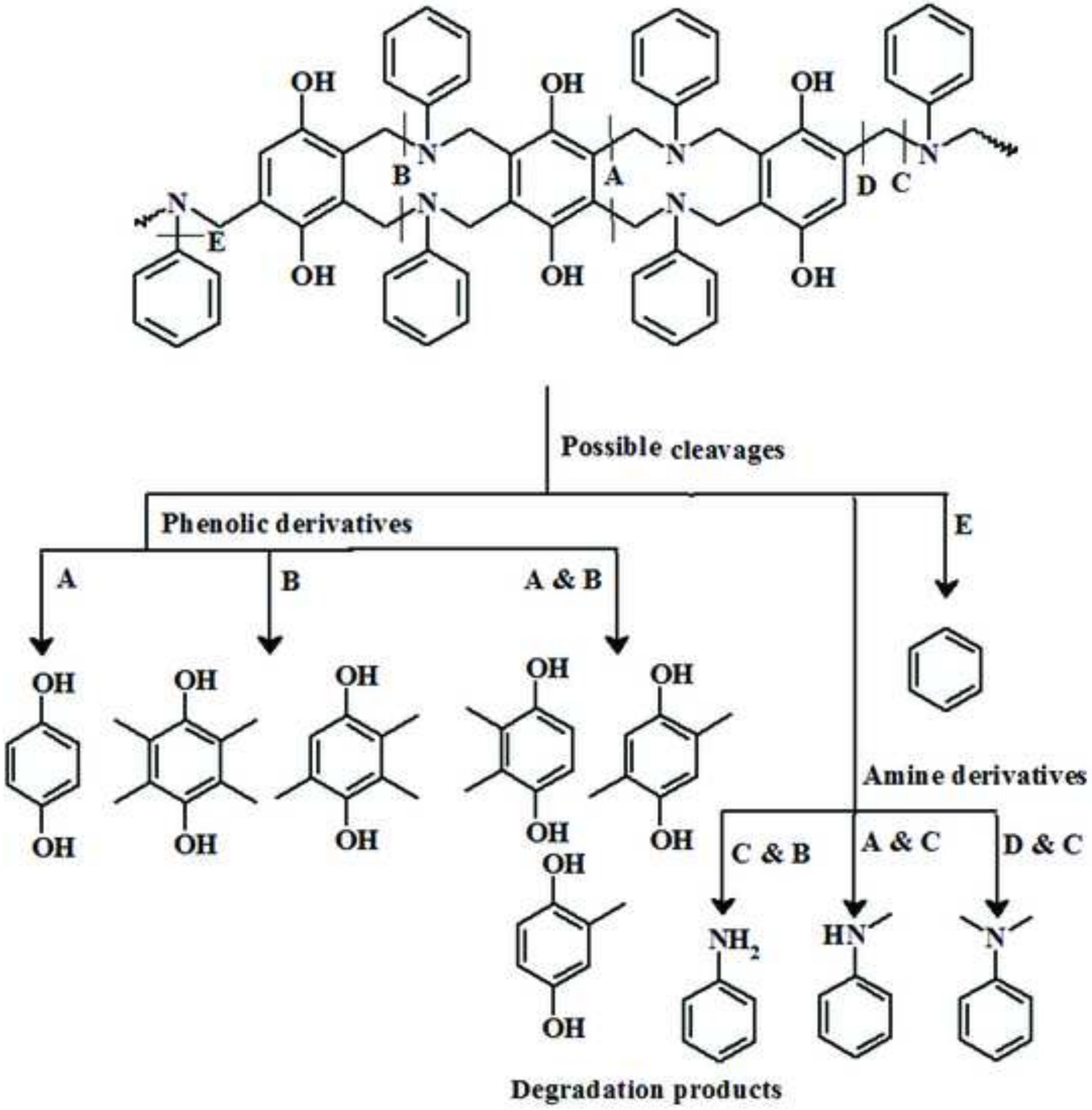
OH
OH
OH
N
N
N
B
A
D
C
N
N
N
E
OH
OH
OH
Possible cleavages
Phenolic derivatives
E
A
B
A & B
OH
OH
OH
OH
OH
OH
OH
OH
OH
OH
OH
OH
Amine derivatives
C & B
A & C
D & C
NH2
HN
N
Degradation products

Figure(s)

Click here to download high resolution image